Performance Analysis for Smart Antennas with Orthogonal Frequency Division Multiplexing Based Wireless Networks

by

Mohammad Qudrat-E-Maula

A thesis submitted to the Department of Electrical and Electronic Engineering of
Bangladesh University of Engineering and Technology
in partial fulfillment of the requirements for the degree of
MASTER OF SCIENCE IN ELECTRICAL AND ELECTRONIC ENGINEERING

DEPARTMENT OF ELECTRICAL AND ELECTRONIC ENGINEERING
BANGLADESH UNIVERSITY OF ENGINEERING AND TECHNOLOGY
July 2005

The thesis titled **"Performance Analysis for Smart Antennas with Orthogonal Frequency Division Multiplexing based Wireless Networks"** submitted by Mohammad Qudrat-E-Maula Roll No: 040306260P, Session: April, 2003 has been accepted as satisfactory in partial fulfillment of the requirements for the degree of **Master of Science in Electrical and Electronic Engineering** on July 05, 2005.

BOARD OF EXAMINERS

1. 05/7/05 — **Chairman**
(Dr. Satya Prasad Majumder)
Professor
Department of Electrical and Electronic Engineering, BUET,
Dhaka-1000, Bangladesh

2. _____ **Member** (Ex-officio)
(Dr. S. Shahnawaz Ahmed)
Professor and Head
Department of Electrical and Electronic Engineering, BUET,
Dhaka-1000, Bangladesh

3. _____ **Member**
(Dr. A. B. M. Siddique Hossain)
Professor
Department of Electrical and Electronic Engineering, BUET,
Dhaka-1000, Bangladesh

4. 05/07/05 — **Member**
(Dr. Md. Saifur Rahman)
Professor
Department of Electrical and Electronic Engineering, BUET,
Dhaka-1000, Bangladesh

5. _____ **Member** (External)
(Mr. Mohammad Abdul Moqaddem)
Divisional Engineer
Bangladesh Telephone and Telegraph Board,
Dhaka, Bangladesh

Declaration

It is hereby declared that this thesis or any part of it has not been submitted elsewhere for the award of any degree or diploma.

Signature of the candidate

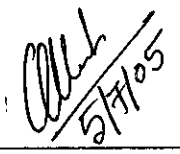

(Mohammad Qudrat-E-Maula)

Dedication

To my parents and wife

Acknowledgements

I would like to express my sincere gratitude to my supervisor Dr. Satya Prasad Majumder for his constant encouragement and supports during this thesis work.

I wish to thank Dr. Fakhrul Alam for his guidance and for sharing his expertise in the orthogonal frequency division multiplexing during the course of this research.

I would also like to thank Mohammad Zulhasnine, Faruk Ahmed for their help with my research.

I would especially like to thank my parents for their encouragement in my quest for higher education and also my wife Shairmina Shafi for her continuous support to finish the thesis successfully.

Contents

List of Tables

List of Figures

List of Principal Symbols

$n(n)$	Additive White Gaussian Noise
E_{avg}	Average Energy of the Signal
$s_m(n)$	Baseband Discrcte Time Signal
U_i	Binary Code Symbol
m_i	Binary Digit
$h(n)$	Channel Impulse Response
$s(n)$	Complete Time Signal
M	Constellation Point
K	Constraint Length
$erf(x)$	Error Function of x
$\gamma_{(J)}$	Gain of the J^{th} Antenna
m	No of Antenna
p_e	Probability of Error
y_m	Received Data Symbol
$r(n)$	Received Time Signal
E_b/N_0	Signal to Noise Ratio
x_m	Transmitted Data Symbol

Abbreviations

AWGN	Additive White Gaussian Noise
BER	Bit Error Rate
BPSK	Binary Phase Shift Keying
COFDM	Coded Orthogonal Frequency Division Multiplexing
CP	Cyclic Prefix
DFT	Discrete Fourier Transform
DSP	Digital Signal Processing
EGC	Equal Gain Combiner
FEC	Forward Error Correction
FFT	Fast Fourier Transform
ICI	Inter Carrier Interference
IDFT	Inverse Discrete Fourier Transform
IFFT	Inverse Fast Fourier Transform
ISI	Inter Symbol Interference
MRC	Maximum Ratio Combiner
MSE	Mean Square Error
MSINR	Maximum Signal-to-Interference Noise Ratio
MSNR	Maximum Signal-to-Noise Ratio
OFDM	Orthogonal Frequency Division Multiplexing
PSK	Phase Shift Keying
QAM	Quadrature Amplitude Modulation
QPSK	Quadrature Phase Shift keying
SIMO	Single Input and Multiple Output
SINR	Signal-to-Interference Noise Ratio
SNR	Signal-to-Noise Ratio
WLAN	Wireless Local Area Network

Abstract

The aim of this thesis work is to design a smart antenna based receiver in an Orthogonal Frequency Division Multiplexing (OFDM) system to improve the system performance and to reduce the computational complexity. OFDM is a special form of multi-carrier transmission that promises a higher data rate and greater resilience to severe signal fading effects at a reasonable level of implementation complexity. OFDM with multiple receiver antennas combine the different receiver signals. This type of OFDM system minimizes fading effects and thereby shows significant improvement in the system performance. However, each of the receivers has its own Fast Fourier Transform (FFT) Block, so the system complexity increases by the combination of receiver signals. To reduce the complexity of the OFDM system, a smart antenna system based Pre-FFT Maximum Ratio Combiner (MRC) is proposed. In the proposed scheme, only one FFT block is used instead of multiple FFT blocks in the receiver end. The received signal are weighted and combined before FFT processing. As a result, the number of FFT blocks reduces and the computational efficiency increases. A mathematical model of the proposed system is developed and the analytical formulation of Bit Error Rate (BER), channel capacity and throughput are also presented. Finally, the performance of the pre-FFT MRC receiver and single receiver are evaluated and compared in terms of BER and other parameters. Computer simulation result shows a significant improvements in Signal-to-Noise Ratio (SNR) for the proposed receiver.

Chapter 1

Introduction

1.1 Introduction

Wireless communication gained popularity in the last decade of the 20^{th} century with the success of 2^{nd} generation (2G) digital cellular mobile services. As a result of the continuous success in the field of wireless communications, 3^{rd} generation (3G) wireless systems with the higher data rate and user mobility have emerged. But 3G is not the end of the tunnel. Ever increasing user demands have drawn the industry to search for better solutions to support higher data rates. Hence, the main focus of the future 4^{th} generation (4G) wireless systems is to support high data rates and to ensure seamless provisioning of services that allow the deployment of multimedia applications. However, in high date rates, the signal waveform is wideband and the channel is frequency selective, that is a large number of resolvable multipaths are present in the environment.

In orthogonal frequency division multiplexing (OFDM), higher data rate data streams are split into a number of lower data rate data streams that are transmitted simultaneously over a number of subcarriers. As the symbol duration increases for the lower rate parallel subcarriers, multipath delay spread is decreased. OFDM is also robust to the frequency selective fading due to the exploitation of a guard interval that is introduced at the beginning of each OFDM symbol. However, once delayed signals beyond the guard interval are introduced in a channel with a large delay spread, inter symbol interference (ISI) causes severe degradation in the transmission performance. A smart antenna array deployed at the receiver is able to enhance the signal integrity in an interference environment [1] thus minimizing ISI. If the desired signals and the interferences are located at different spatial locations, the antenna array can act as a spatial filter which

separates the desired signal from the interferences. In the wireless environment, using a smart antenna can reduce the co-channel interferences from other users within its own cell and the neighboring cells, thus increasing the system capacity [2]. Due to its advantages, a smart antenna array is likely to be an integral part of the 4G systems.

The application of adaptive algorithms in the antenna array for the single-carrier systems has been studied extensively. However, there are relatively few technical papers on OFDM systems applying smart antennas and investigating interference suppression capability for multipath environments. The nature of modulation/demodulation on subcarriers in an OFDM system requires a new approach for implementing adaptive algorithms in the antenna array. Therefore, it is necessary to understand the fundamental principle of OFDM and to develop techniques for applying adaptive array algorithms to OFDM systems.

1.2 Literature Review

In this section, the previous works on OFDM and smart antennas are briefly presented. Research on vector channel models which investigate the performance of a receiver equipped with smart antenna [3] are also presented.

The origins of OFDM development started in the late 1950's with the introduction of frequency division multiplexing (FDM) for data communications. The concept of multi-carrier transmission was introduced since 1960s [4] and the patent for OFDM was issued in the beginning of 1970 [5]. In 1971, Weinstein [6] introduced the idea of using a discrete fourier transform (DFT) for implementation of the generation and reception of OFDM signals, eliminating the requirement for banks of analog subcarrier oscillators. This idea commenced an opportunity to implement OFDM with the use of fast fourier transform (FFT), which is an efficient implementation of the DFT. OFDM was studied during the 1980s for high speed modems [7]. The research on OFDM gained momentum in the 1990s. The loss of orthogonality due to the doppler spread has been analyzed in [8]. The effects of inter-carrier interference (ICI) and ISI and the techniques to combat these detrimental phenomena have been investigated in [9]-[10].

Research on adaptive antenna systems for wireless communications dates back to the 1960s [11]-[12]. Adaptive antenna receivers provide spatial diversity and

are considered to be the last frontier to improve data rates without the necessity of additional spectrum. An adaptive antenna array has been proposed to increase the capacity of an OFDM based system [13]. Co-Channel interference (CCI) cancellation with the aid of a minimum mean square error (MMSE) based adaptive antenna array has been demonstrated in [14]. Combined diversity and beamforming have been shown to be effective to combat ICI and ISI in a slow varying channel [15]. Time domain beamforming for an OFDM receiver based on Least Mean Square (LMS) driven MMSE beamforming has been proposed in [16]. MMSE based adaptive antenna has also been proposed [17] to suppress the delayed signal and doppler shifted signal. Optimum beamforming for Pre-FFT OFDM adaptive antenna array is proposed in [18] and Pre-DFT processing using eigenanalysis for OFDM with multiple antennas are proposed in [19].

Vector channel models are used to investigate the performance of a receiver. These models describe the temporal or spectral parameters like power delay profile, doppler spread as well as spatial parameters like angle of arrival (AOA) and angle spread etc. Geometrically based vector channel models define a region in space where the objects are distributed and the distribution of these objects are responsible for scattering and/or reflection. Circular channel model [20] is a popular model to describe the macro-cellular environment. In a circular channel model the transmitter is surrounded by local scatterers that are distributed within a circle centered on the transmitter. Typical urban models are special cases of the circular channel model [21]. The elliptical channel model [22] provides a much greater angle spread than the previously mentioned models. There are other geometrical models that can be found in the literature [23]. There is also a separate class of vector channel models known as the statistical vector channel model that can be found in the literature [24]. A special statistical channel model based on the Jakes model [25] can be employed to generate the complex coefficient of a resolvable multipath as a summation of a number of unresolvable components. This model provides very good control over the angle spread of the unresolvable components.

1.3 Objectives of the Thesis

In this thesis, smart antennas with OFDM based wireless network is introduced. Usually, A single antenna is used at the transmitter and receiver end of the OFDM model. In the proposed OFDM model, multiple smart antennas are used at the receiver end. Signals received by the multiple receiver antennas are combined by the maximum ratio combining methods. As the combining process takes place before the FFT processing at the receiver, only one FFT block is needed at the receiver and thus, minimizing the computational complexity of the receiver. The proposed model is applied in the indoor environment. Hence, a statistical channel model based on the modified Jake's model is used in the simulation.

1.4 Thesis Overview

The remaining chapters of this thesis are organized as follows:

In chapter 2, the concepts of smart antennas such as phased arrays and diversity arrays are introduced. The basic combining techniques of smart antennas such as diversity and beamforming are presented and also compared.

In chapter 3, the concepts of OFDM with block diagrams are discussed. Each block of OFDM system employing single antenna at the transmitter and receiver ends are discussed in detail.

In chapter 4, the proposed model of the OFDM receiver with multiple antennas are presented. A mathematical analysis of the proposed system and a theoretical analysis of the BER is also presented. Finally, the channel used in the proposed model is also discussed.

In Chapter 5, simulation results are presented with detail discussion. Single and multiple smart antennas are compared to show the superiority of the proposed method.

Chapter 6 summarizes the results of the research works and give further research directions.

Chapter 2

Smart Antenna

The necessity to improve the capacity of wireless communication systems has led to the need for exploiting the spatial characteristics of the wireless channel. An effective means to exploit the spatial dimension is through the use of adaptive antenna arrays also referred to as intelligent antennas or smart antennas [26]. A lot of research has been done to improve the capacity of the wireless systems due to the use of smart antennas. In this chapter, some of the basic concepts of smart antennas are discussed.

2.1 Introduction

The two main factors that make wireless communications difficult are the presence of the multipath fading and the co-channel interference. The use of smart antennas can improve performance in these hostile environments. Smart antennas can be classified into two categories, namely the phased array and the diversity array. Elements in a phased array are placed at a distance less than or equal to half of a wavelength while those in a diversity array are placed at a much larger distance. As a result, the assumption that the received signal is a plane waves holds true for a phased array but not for a diversity array.

2.2 Antenna Array

Smart antennas use an array of a low gain antenna elements that are connected by a combining network. The array may consist of a number of antenna elements arranged in a desired pattern: linear equally spaced (LES), uniform circular, or uniformly spaced planar array of similar, co-polarized, low-gain elements which

are oriented in the same direction.

2.2.1 Why Antenna Array?

The use of antenna arrays at the receiver in wireless data networks may be motivated in several ways:

1. Array gain: By using antenna arrays, it is possible to combine the signals so that the SNR is improved.

2. Fading diversity: Due to the multipath propagation, several replicas of the transmitted message may be incidenton the receiving antennas. The interference between the incident waves that cause the signal level to change is known as fading. By using several antennas, the reliability increases, as it is not likely for the multiple received signals at the different elements of the array to suffer the same distortion.

3. Interference suppression: In the spatial dimension, signals that have the same temporal properties and occupy the same frequency band may have different propagation paths, coming from different space locations. By using the spatial processing, it is possible to suppress interferences in a way that is not possible using a single antenna.

4. Transmitter localization: The use of antenna arrays at the receiver may be used to calculate parameters such as the direction of arrival of the incident waves. This information is useful for interference suppression and could be used for emergency localization.

The antenna arrays are also used in transmission. Using space-time processing, the induced currents into the antenna elements can focus the antenna pattern towards a desired user, while minimizing the interference of other users. Antenna arrays also provide extended coverage and higher data rates than conventional antenna systems.

2.3 Phased Array and Diversity Array

A phased array consists of a set of antenna elements that are spatially distributed at known locations with reference to a common fixed point. By changing the

phase and amplitude of the exciting currents in each of the antenna elements, it is possible to create gains and nulls in any direction, [27]. The signals received in these elements are typically combined at baseband using complex weights. Adaptive algorithms can be used to adapt the weights based on some optimization criteria such as the maximization of the output SNR. Also there are algorithms by which the output signal-to-interference noise ratio (SINR) can be maximized. In such a system, the antenna response is maximized in the direction of the desired user and is minimized in the direction of the interferer.

Phased arrays are typically used for interference rejection while diversity arrays are used for combating multipath fading in mobile wireless channels. In diversity arrays, the elements are spaced sufficiently apart so that the fading envelopes seen at the antenna elements are uncorrelated or slightly correlated. The main idea behind diversity arrays is that such uncorrelated (or slightly correlated) branches will have very low probability of simultaneously experiencing a deep fade. Thus having more elements increases the probability that at least one element will produce sufficient SNR for reliable decoding of the information. Additionally, in diversity arrays there is no geometric interpretation of the array response and the concept of beam pattern is invalid. However, a very important result is that the combining approaches used in diversity arrays are similar to the beamforming approaches used in phased arrays because several of these algorithms have the same maximization criteria. Thus the weights used in phased arrays to maximize the SNR are simply the same as the maximum ratio combiner (MRC) solution for diversity arrays.

Various array geometries are possible for the antenna elements with the most common of them being linear, circular and planar arrays. In a linear array, the centers of all array elements are aligned in a straight line. If the spacing between the elements is uniform it is called a uniformly spaced linear array. A circular array is one in which the centers of the array elements lie on a circle. On the other hand if the centers of the array elements all lie in the same plane it is called a planar array. Linear and circular arrays are special cases of the planar array.

The radiation pattern of the array is determined by the radiation patterns of the individual elements, their orientation in space and the amplitude and phase of the feeding currents. If each elementof the array is an isotropic source, the radiation pattern obtained will be solely dependenton the array geometry and

the feeding currents. The radiation pattern thus obtained is called the array factor. If the elements of the array are similar and if they are non-isotropic, the radiation pattern is computed from the principle of pattern multiplication as the product of the array factor and the individual element pattern [28]. In this thesis, a uniform linear array is considered.

2.4 Uniform Linear Array

If the spacing between the elements of a linear array is equal, it is known as uniform linear array (ULA). Figure 2.1 shows a K element ULA. The spacing between the array elements is d and a plane wave arrives at the array from a direction θ off the array broadside. The array broadside is perpendicular to the line containing the center of the elements. The angle θ measured clockwise from the array broadside is called the direction of arrival (DOA) or the angle of arrival (AOA) of the received signal. The received signal at the first element can be

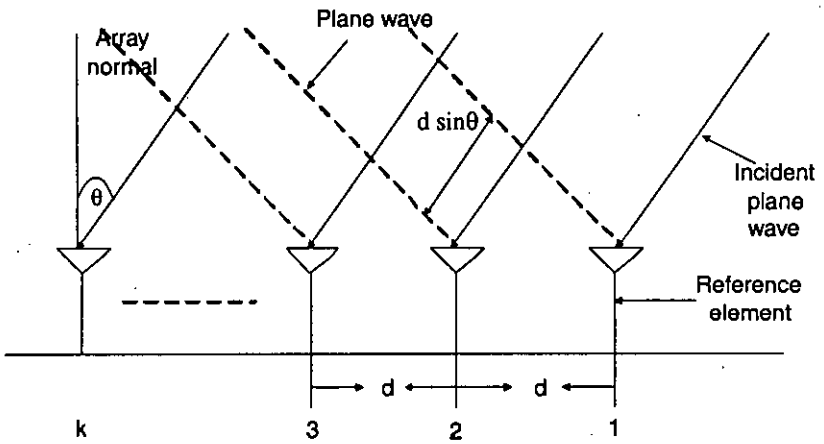

Figure 2.1: A uniformly spaced linear antenna array

written as [31]

$$\hat{x}_1(t) = A_1(t)\cos[2\pi f_c t + \gamma(t) + \beta] \tag{2.1}$$

where,

$A_1(t)$ is the amplitude of the signal.

f_c is the carrier frequency.

$\gamma(t)$ is the information.

β is the random phase. Note that the complex envelope of the signal at the first element is given by

$$\hat{x}_1(t) = A_1(t)e^{j[\gamma(t)+\beta]} \tag{2.2}$$

Let us assume that the signals originate far away from the array and the plane wave associated with the signal advances through a non-dispersive medium that only introduces propagation delay. Under these circumstances, the signal at any other element can be represented by a time advanced or time- delayed version of the signal at the first element. Referring to Figure 2.1, the wave front impinging on the first element travels an additional $dsin\theta$ distance to arrive at the second element. The time delay due to this additional propagation distance is given by

$$\tau = \frac{d\sin\theta}{c} \tag{2.3}$$

where c is the velocity of light. The signal at the second element is thus given by

$$\hat{x}_2(t) = \hat{x}_1(t-\tau) = A_1(t-\tau)\cos[2\pi f_c(t-\tau) + \gamma(t-\tau) + \beta] \tag{2.4}$$

If the carrier frequency f_c is large compared to the bandwidth of the impinging signal, the signal may be treated as quasi-static during time intervals of order τ and it can be written

$$\hat{x}_2(t) = A(t)\cos[2\pi f_c t - 2\pi f_c \tau + \gamma(t) + \beta] \tag{2.5}$$

Thus the complex envelope of the signal at the second antenna can be written as

$$\begin{aligned} x_2(t) &= A(t)e^{j[-2\pi f_c\tau+\gamma(t)+\beta]} \\ &= x_1(t)e^{j[-2\pi f_c\tau]} \end{aligned} \tag{2.6}$$

It is thus evident from Equation (2.6) that the time delay of the signal can now be represented by a phase shift. From Equations (2.3) and (2.6), it can be written

$$\begin{aligned} x_2(t) &= x_1(t)e^{j[-2\pi f_c \frac{d\sin\theta}{c}]} \\ &= x_1(t)e^{-j[2\pi \frac{d\sin\theta}{\lambda}]} \end{aligned} \tag{2.7}$$

Therefore the complex envelope of the received signal at the $i^{th}(i = 1, 2, ., K)$ element can be expressed as

$$x_i(t) = x_1(t)e^{-j[2\pi \frac{d(i-1)\sin\theta}{\lambda}]} \tag{2.8}$$

Let a column vector is defined whose each element contains the received signal at the corresponding array element. Therefore the received signal vector is defined as

$$\mathbf{x}(t) = [x_1(t) \quad x_2(t) \quad \ldots\ldots \quad x_K(t)] \tag{2.9}$$

where T represents transpose.
It can be also define

$$\mathbf{a}(\theta) = [1 \quad e^{-j[2\pi \frac{d\sin\theta}{\lambda}]} \quad \ldots\ldots \quad e^{-j[2\pi \frac{d(K-1)\sin\theta}{\lambda}]}]^T \tag{2.10}$$

$\mathbf{a}(\theta)$is known as the array response vector or the steering vector of an ULA. The array response vector is a function of the AOA, individual element response, the array geometry and the signal frequency. It will be assume that for the range of operating carrier frequency, the array response vector does not change. Since, the geometry (uniform linear array) and the individual element response (identical isotropic elements) have already fixed, the array response vector is a function of the AOA only. The received signal vector can now be written in a compact vector form as

$$\mathbf{x}(t) = \mathbf{a}(\theta)x(t) \tag{2.11}$$

It is assumed that the bandwidth of the impinging signal is much smaller than the reciprocal of the propagation time across the array. This assumption, commonly known as the narrowband assumption [29] for the signal, made it possible to represent the propagation delay within the elements of the array by phase shifts in the signal. Although the narrowband model is exact for sinusoidal signals, this is usually a good approximation for a situation where the bandwidth of the signal is very small compared to the inverse of the propagation time across the array. Any deviation from the narrowband model is detrimental to the performance of a narrowband beamformer usually manifesting as a limit in the ability to null interferers [30]. In such a scenario, a wideband beamformer [31] must be used.

2.5 Smart Antenna Array

In wireless environments, the users keep moving and hence, the DOAs of the users are time-varying. Also the parameters of the user's signals vary in time

due to the presence of co-channel interference, noise and multipath associated with the channel. Fixed weights will not track these changes in the time varying channel. An adaptive antenna array can change its beam pattern in response to the changing signals. This kind of an antenna system usually works with some internal feedback whereby the system can modify the antenna patterns. The weights used must be changed using some adaptive algorithm. Such algorithms are usually designed to meet some performance criteria and then generating a set of equations such that the performance criteria are met. Some of the most frequently used performance criteria are the mean square error (MSE), the maximum likelihood (ML), maximum signal-to-noise ratio (MSNR) and maximum signal-to-interference noise ratio (MSINR). These performance criteria are usually expressed as cost functions and the weights are adapted iteratively until the cost functions converge to a minimum value. Once the cost function is minimized it can be assured that the performance criterion is met and the algorithm is said to have converged. There are several factors that are to be considered while choosing an adaptive algorithm like the convergence rate of the algorithm, complexity and robustness. The convergence rate is the number of iterations required for the convergence of the algorithm. In wireless environments, convergence rate is important as it is important to converge to optimum before the channel conditions change. The complexity issues come into play when it is needed to determine the number of digital signal processing (DSP) cycles needed for algorithm implementation. Finally the algorithm one can choose might be robust as it should be able to perform fairly well even in the cases where the input data may be ill-conditioned.

2.5.1 Theoretical Model

The adaptive antenna system needs to differentiate the desired signal from the co-channel interferences. It requires a reference signal, a training signal or the direction of the desired signal source (direction of arrival) to achieve its objectives [32]. There are a number of existing schemes to estimate the direction of arrival and methods of updating the array weights. Algorithms also exist that exploit properties of signal to eliminate the need of training signals.

The overall pattern of the antenna array is determined by the radiation pattern of the individual elements, their position, their orientation in space, and the

relativep hase and amplitude of the feeding currents to the elements. By the principle of pattern multiplication, the total field pattern of the array $F(\theta, \phi)$ is given by the product of the array factor $f(\theta, \phi)$ and the individual element radiation pattern $g_a(\theta, \phi)$:

$$F(\theta, \phi) = f(\theta, \phi) \times g_a(\theta, \phi) \tag{2.12}$$

where ϕ is the azimuthal angle and θ is the elevation angle of a plane wave incident on the array. The pair (θ, ϕ) is referred to as the direction of arrival. The relative positions of the elements as well as the relative phase and amplitudes of the feeding currents into the elements in turn determine the array factor. The array factor and therefore the radiation pattern of the array can be continuously adapted by adjusting the relative phases and amplitudes of the feeding currents at the elements.

Each branch of the array has a weighing element w_m. The weighing element w_m, has both magnitude and phase. By adjusting the set of weights, w_m, it is possible to direct the main beam of the array factor in any desired direction (θ_o, ϕ_o). The array shown in Figure 2.2 has a reference element at the origin and

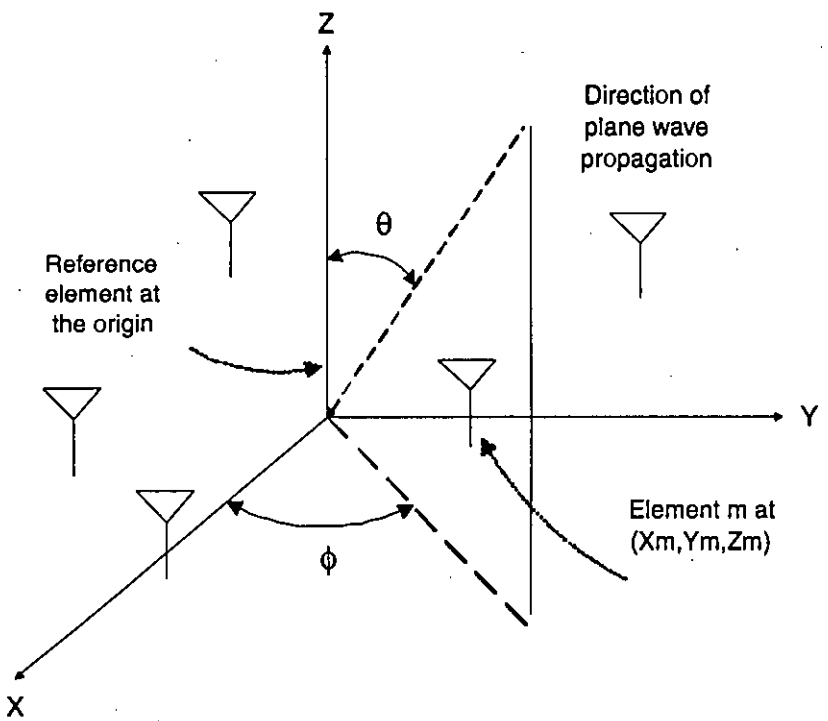

Figure 2.2: Co-ordinates of an antenna array

the coordinates of the m^{th} element are (x_m, y_m, z_m). When working with antenna arrays it is helpful to make use of vectors and matrices. The weight vector of an antenna array is defined as:

$$w = [w_0 w_1 w_2 .....w_{M-1}]^H \quad where \;\; w_m = e^{j\beta_m \Delta d cos\phi_0} \tag{2.13}$$

where the H superscript represents the Hermitian transpose, which is a transposition combined with complex conjugation. The signals from each antenna element are grouped in a data vector:

$$u = [u_0(t) u_1(t) u_2(t) .....u_{M-1}(t)]^H \;\; where \;\; u_0(t) = As(t)e^{-j\beta_m \Delta d cos\phi_0 sin\theta} \tag{2.14}$$

Then the product of the array vector w and the data vector u(t) gives the array output:

$$z(t) = w^H u(t) \tag{2.15}$$

and the array factor in a direction (θ, ϕ) is:

$$f(\theta, \phi) = w^H a(\theta, \phi) \tag{2.16}$$

The vector $a(\theta, \phi)$ is called the steering vector in direction θ, ϕ. Given there is a plan wave incident from a direction θ, ϕ, the steering vector $a(\theta, \phi)$ describes the phase of the signal at each of the antenna elements relative to the phase signal of the reference element (element 0).

$$a(\theta, \phi) = [1 \quad a_1(\theta, \phi) .....a_{M-1}(\theta, \phi)]^T \tag{2.17}$$

difference between the m^{th} element and the reference element of the antenna array and $\beta = 2\pi/\lambda$ is the wave number. The characteristics of an array are defined by the size and the arrangement of the antenna elements. The size of the antenna array or the array aperture determines the gain the antenna array can achieve. The number of elements in an array determines the degrees of freedom of the array. The spacing of the elements plays also an important role in designing the antenna array. For a linear equally spaced (LES) array if the spacing between elements exceeds $\lambda/2$, then grating lobes can appear, giving the array undesired beams, which may amplify noise or interference.

However, non-uniform spacing can also be used in design. These non-uniform spaced arrays, known as sparse-arrays, can yield larger apertures and smaller beamwidth that the half-wavelength spaced arrays of similar complexity at the expense of size.

2.6 Diversity

In the mobile communications channel, multipath can lead to fading in the received signal, especially when the signal bandwidth is small compared to the coherence bandwidth of the channcl. Spatial diversity provides an effective and economical means of reducing narrowband fading.

Fading is most severe in heavily built-up areas in an urban environment. Buildings and various obstacles scatter the propagating signal, and because of the interaction of the different waves arriving at the antenna, the resultant signal received by the antenna system is subject (suffers) to rapid and deep fading. The signal envelope has a Rayleigh distribution over short distances and a log-normal distribution over large distances. Diversity reception techniques are used to reduce the effects of fading. In principle, diversity reception techniques can be applied either at the base-station or at the mobile, although different problems have to be solved.

The basic idea of a diversity reception is that, if two or more independent samples of a signal are taken, then these samples will fade in an uncorrelated manner. This means that the probability that all signal samples being simultaneously below a given level is much less than the probability of any individual sample being below that level. The probability of M samples all being under a certain level is pM, where p is the probability that a single sample is below the level. It can be shown that a signal composed of a suitable combination of the various samples will suffer much less severe fading than any individual sample alone.

There are many types of diversity combining techniques. Some of them are: 1. Selection combiner 2. Maximum ratio combiner 3. Equal gain combiner 4. Optimum combiner.

2.6.1 Selection Combiner

The selection combining is the simplest of all diversity schemes. The selection combiner chooses the signal with the highest instantaneous power of SIR, so the output SIR is equal to that of the best incoming signal. However, due to the fact that systems can not get instantaneous values, for the system to operate efficiently the internal time constants have to be considerably shorter than the

fading periods. To avoid the system complexity associated with estimating SNR of each branch, most practical systems monitor only the currently selected branchs SNR and then switch branches only the SNR drops below a certain threshold. This technique is referred to as switched diversity. Figure 2.3 shows the block diagram of a selection combiner.

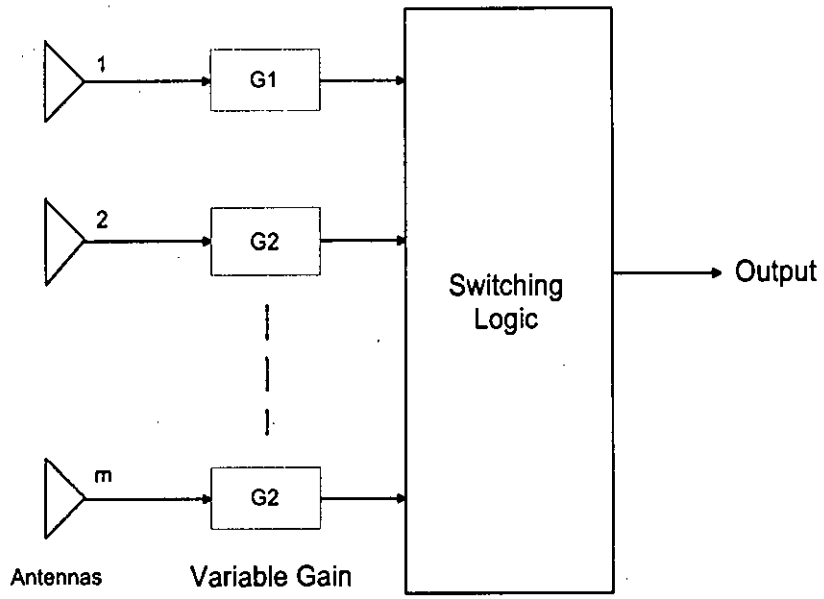

Figure 2.3: Block diagram of a selection combiner

2.6.2 Maximum Ratio Combiner

Another used technique is the maximum ratio combiner (MRC), which adjusts both the magnitude and the phase of weights in the combining network to maximize the SNR at the output of the combiner. An MRC system could be implemented as an adaptive array, whose antenna elements are widely separated. In an interference-free environment, an MRC array could also be implemented as an adaptive array without using feedback from the array output to adjust amplitude weighing of each branch. In such an MRC implementation, the multiple array signals are weighed proportional to their signal-to-noise power ratios and then summed. While an MRC array can achieve optimal performance in the presence of noise, it does not provide the ability to reject interference or multipath. Figure 2.4 shows the block diagram of a maximum ratio combiner.

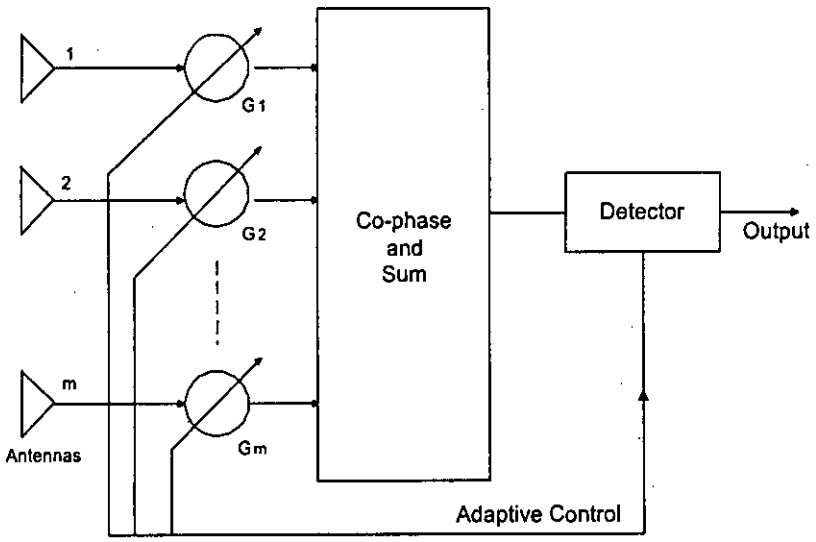

Figure 2.4: Block diagram of a maximal ratio combiner

2.6.3 Equal Gain Combiner

Equal gain combiner is a diversity technique in which the desired signals present at each antenna element are co-phased and then added together. There is no attempt to weigh the signals before addition. As a result of this there is no need to estimate the SNR at each branch. The performance lost using equal gain combining when compared to MRC is approximately 1dB.

2.6.4 Optimum Combiner

Optimum combiner refers to the diversity method, which yields the maximum output SINR. This is identical to using MRC when the noise and interference are white. However, in the presence of correlated interference, the optimal combiner will try to maximize SNR and reduce interference. The performance gained by using optimum combining as compared to MRC is highly dependent upon the properties of the signals. The optimization criterion can include maximizing SNR, maximizing the SINR, minimizing the mean square error (MMSE) between the received signal and a reference signal, the minimum variance distortionless response (MVDR).

2.7 Beamforming

In wireless environments it is often seen that the desired signal and the interference occupy the same frequency band. Unless the signals have low correlation (like in CDMA systems), temporal processing will not be effective in interference rejection. However the desired signal and the interference arrive from different directions and hence have different angle of arrival. Beamforming is the process of forming beams towards the direction of the desired user while simultaneously suppressing signals originating from other directions, given that they have same frequency band. Thus beamforming can also be looked upon as the spatial filtering of signals using their spatial signature properties.

A beamformer combines sampled data from each antenna element the same way an FIR filter would combine temporally sampled information. Beamformers are of three general types, a conventional beamformer, a narrowband beamformer and a wideband beamformer.

2.7.1 Conventional Beamformer

Adjusting only the phase of the signals from different antenna elements to point a beam in a desired direction is the conventional method of beam pointing or beam forming. The gain of each signal is kept the same. This determines the total gain of the array in the beam pointing direction. The shape of the antenna pattern in this case is fixed, that is, the positions of the side-lobes with respect to the main lobe remain unchanged. In other words, the main beam is steered in different directions by adjusting various phases, but the positions of the side-lobes relative to the main lobe do not change. However, this may be changed by adjusting both the gain and phase of each signal to shape the pattern as required. The amount of change depends on the number of elements of the array. The gain and phase applied to the signals, derived from each element may be represented as a single complex quantity, referred to as the weighing applied to signals. With an N element array one is able to specify N-1 positions. These may be one maxima in the direction of the signal-of-interest (SOI) and N-1 nulls in the directions of the interferers.

2.7.2 Narrowband Beamformer

A narrowband beamformer is shown in the Figure 2.5. A narrowband signal sampled at the i-th antenna element at time k is just the phase-shifted version of the signal received at the reference antenna element at time k. Since this phase shift is a function of the distance between the first antenna element and the $i-th$ antenna element, a narrowband beamformer needs to sample the propagating wave field in space only. The signal at the output of the beamformer at time k,

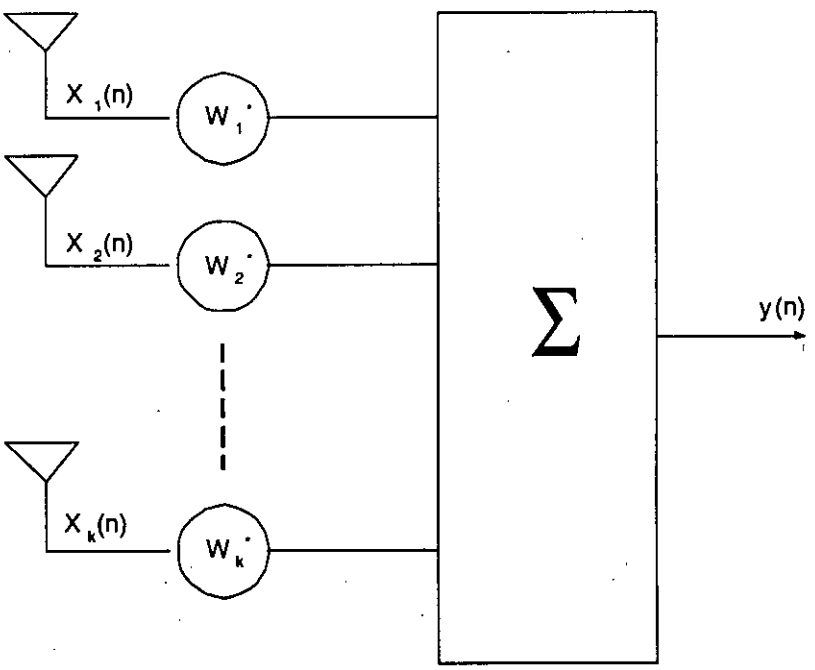

Figure 2.5: Narrowband beamforming

y(k), is given by a linear combination of the data at the K sensors at time k. The output of the beamformer is given by,

$$y(n) = \sum_{k=1}^{K} w_k^* x_k(n) \tag{2.18}$$

where the complex weights w are used to steer the beam towards the desired user and steer nulls towards interferers. The above equation can be written in vector form as

$$y(n) = \mathbf{w}^H \mathbf{x}(n) \tag{2.19}$$

Where H denotes the Hermitian (complex conjugate) transpose and

$$\mathbf{w} = [w_1, w_2, ..., w_k]^T \tag{2.20}$$

is the complex weight vector.

2.7.3 Wideband Beamformer

A wideband beamformer is often used when signals of wide band are of interest and is more complex than a narrow band beamformer [1]. Figure 2.6 shows a wideband beamformer. A wideband signal sampled at the $k-th$ antenna element at time n is not just only a phase shift but also time delayed with respect to the signal received at the reference antenna element sampled at time n. This requires

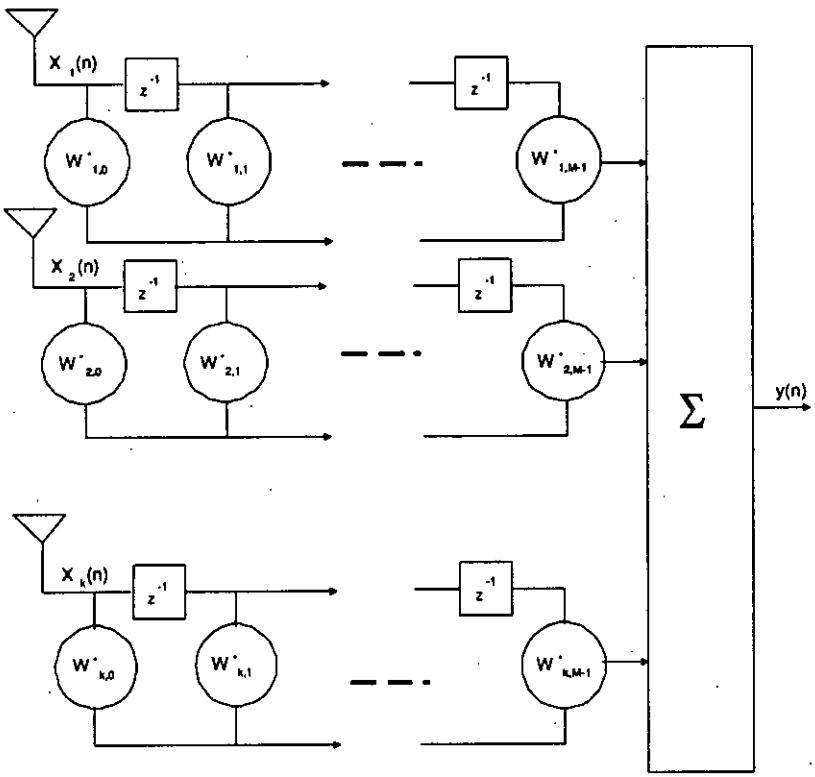

Figure 2.6: Wideband beamforming

a wideband beamformer to sample the propagating wave field in both space and time. The output of a wideband beamformer can be expressed as

$$y(n) = \sum_{k=1}^{K} \sum_{m=0}^{M-1} w_{k,m}^{*} x_k(n-m) \tag{2.21}$$

where $M-1$ is the number of delays in each of the M sensor channels. Equation (2.21) can also be expressed in vector form as in Equation (2.19), where

$$\mathbf{w} = [w_{1,0}, ..., w_{1,M-1}, ..., w_{k,0}, ..., w_{k,M-1}]^T \tag{2.22}$$

and

$$\mathbf{x}(n) = [x_1(n), ..., x_1(n-M+1), ..., x_k(n), ..., x_k(n-M+1)]^T \quad (2.23)$$

In this case, both $\mathbf{w}$ and $\mathbf{x}(n)$ are $KM \times 1$ column vectors.

The wideband beamformer shown in Figure 2.6 is more complex than the narrowband beamformer shown in Figure 2.5. To reduce the complexity, a wideband beamformer can be implemented in the frequency domain. The signal received at the k-th antenna element has a phase shift of $(2\pi/\lambda)(k-1)dsin\theta$ with respect to the signal received at the reference antenna element. For wideband signals, the frequency components at the two edges of the band may be widely different. Since $\lambda = c/f$, their corresponding wavelengths can be widely different and thus the phase shifts experienced by the frequency components at the two edges of the band are not equal. Therefore, it is intuitive that a wideband signal can be decomposed into frequency components and data at each frequency component is processed by its own beamformer.

2.8 Diversity Versus Beamforming

Smart antennas can exploit diversity or beamforming. For diversity, one rely essentially on the statistical independence of the signals at the different antenna elements. In the simplest case, one can exploit the fact that it is very improbable that the signals of all elements are simultaneously in a dip fading, by choosing the signal from the antenna with the highest field strength. More advanced versions of diversity algorithms combine the signals with such weights that the SNIR is optimized. For beamforming, one can exploit the fact that the antenna elements are close together so that appreciable coherence between the antenna signals is present. The closeness of the antenna elements allows us to form an antenna pattern with a single main beam that enhances the desired signal and suppresses the interference. Mathematically speaking, the difference between diversity and beamforming is not dramatic, since both cases combine signals linearly. However, the weight adaptation algorithms are usually quite different.

2.9 Summary

In this chapter, the basic concept of the antenna array and the adaptive antenna array or smart antennas is introduced. Here diversity and beamforming techniques are also introduced which are used as a signal combining technique in smart antennas. This chapter concludes with the comparison between the diversity and beamforming, and shows that they are virtually the similar combining techniques.

Chapter 3

Orthogonal Frequency Division Multiplexing (OFDM)

The orthogonal frequency division multiplexing (OFDM) is based on the multicarrier transmissions technique. The idea of multicarrier transmissions is to divide the total signal bandwidth into a number of subcarriers and information is transmitted on each of the subcarriers. In the conventional multicarrier communication schemes, the spectrum of each subcarrier is non-overlapping and the bandpass filtering is used to extract the desired frequency band. Whereas, in OFDM, the frequency spacing between subcarriers is selected such that the subcarriers are mathematically orthogonal to each other. The spectra of subcarriers overlaps each other but individual subcarriers can be extracted by baseband processing. This overlapping property makes the OFDM more spectral efficient than the conventional multicarrier communication scheme.

3.1 Introduction

The basic principle of OFDM is to split high data stream into a number of lower data stream that are transmitted simultaneously over a number of subcarriers. As symbol duration increases for lower rate parallel subcarriers, the relative amount of dispersion caused by multipath delay spread is decreased. In OFDM, ISI and ICI are eliminated almost completely by introducing a guard time. Further in OFDM multiple receiver antenna can be used to improve system performance. Before going to the discussion on OFDM transmitter and receiver, the concept of multicarrier modulation and orthogonality is discussed.

3.1.1 Multicarrier Modulation

In single carrier modulation, data is sent serially over the channel by modulating one single carrier at a rate of R symbols per second. The data symbol T_s is then $1/R$. In a multipath fading channel, the time dispersion can be significant compared to the symbol period, which results in ISI. A complex equalizer is then needed to compensate for the channel distortion.

In multicarrier modulation the available bandwidth W is divided into a number of N_c of subbands, commonly called subcarriers, each of width $\Delta f = W/N_c$. The subdivision of the bandwidth is illustrated in Figure 3.1, where arrows represent the different subcarriers. Instead of transmitting the data symbols in a serial way, at a rate of R, multicarrier transmitter partitions the data stream into blocks of N_c data symbols that are transmitted in parallel by modulating the N_c carriers. The symbol duration for a multicarrier scheme is $T_s = N_c/R$.

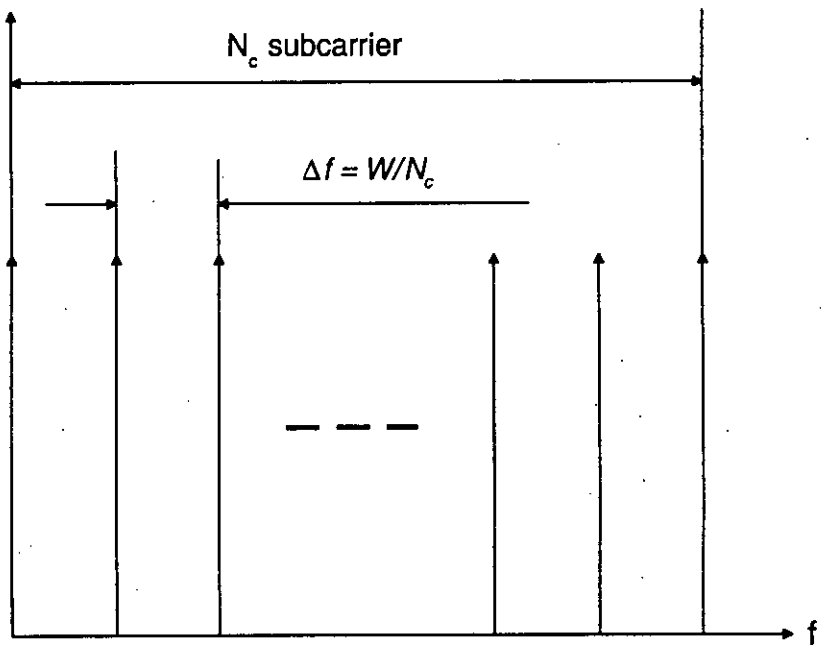

Figure 3.1: Subdivision of the bandwidth into Nc subbands

In its most general form, the multicarrier signal can be written as a set of modulated carriers:

$$s(t) = \sum_{m=-\infty}^{+\infty} \left(\sum_{k=0}^{N_c-1} x_{k,m} \Psi_k(t - mT_s) \right) \tag{3.1}$$

where $x_{k,m}$ is the data symbol modulating the k^{th} subcarrier in the m^{th} signalling interval. Ψ is the waveform for the k^{th} subcarrier.

The symbol duration can bemade long compared to the maximum excess delay of the channel or $T_s >> \tau_{max}$, by choosing N_c sufficiently high. At the same time the bandwidth of the subbands can be made small compared to the coherence bandwidth of the channel $B_{coh} >> W/N_c$. The subbands then experience flat fading, which reduces equalization to single complex multiplication per carrier.

Increasing N_c thus reduces the ISI and simplifies the equalizer into a single multiplication. However, the performance in time variant channels is degraded by long symbols. If the coherence time T_{coh} of the channel is small compared to T_s, the channel frequency response changes significantly during the transmission of one symbol and a reliable detection of the transmitted information becomes impossible. As a consequence, the coherence time of the channel defines an upper bound for the number of subcarriers.

3.1.2 Orthogonality

Orthogonality is a property that allows multiple signals to be transmitted perfectly over a common channel and detected, without interference. Signals are orthogonal if they are mutually independent of each other. In the frequency domain most frequency division multiplexing (FDM) systems are orthogonal as each of the separate transmission signals are well spaced out in frequency preventing interference. But the term OFDM has been reserved for a special form of FDM. The subcarriers in an OFDM signal are spaced as close as is theoretically possible while maintaining orthogonality between them. OFDM achieves orthogonality in the frequency domain by allocating each of the separate information signals onto different subcarriers. OFDM signals are made up from a sum of sinusoids, with each corresponding to a subcarrier. The baseband frequency of each subcarrier is chosen to be an integer multiple of the inverse of the symbol time, resulting in all subcarriers having an integer number of cycles per symbol. As a consequence the subcarriers are orthogonal to each other. Figure 3.2 shows the construction of an OFDM signal with four subcarriers.

Sets of functions are orthogonal to each other if they match the conditions in Equation (3.2). If any two different functions within the set are multiplied, and integrated over a symbol period, the result is zero, for orthogonal functions.

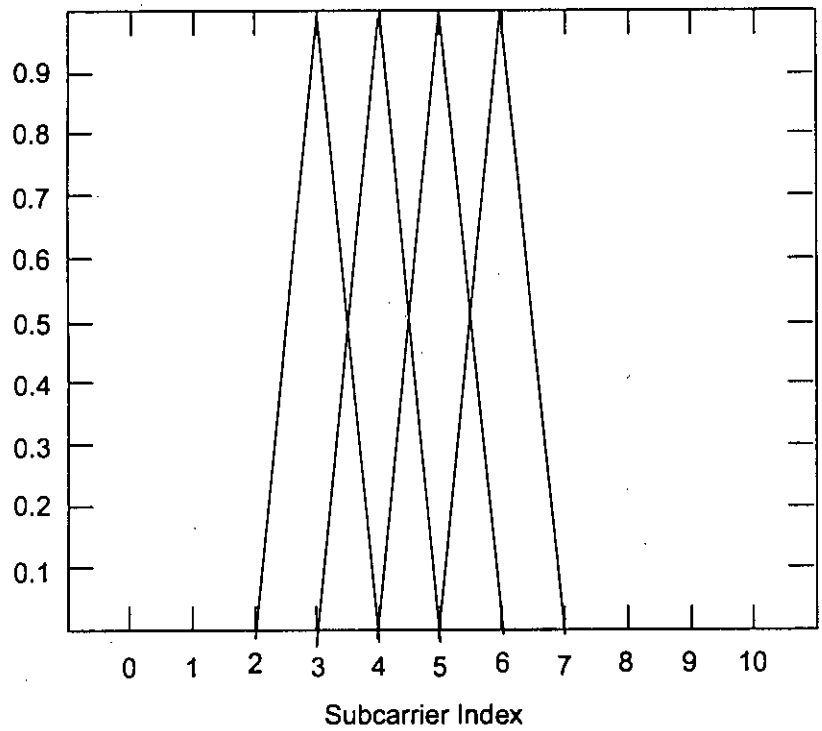

Figure 3.2: Spectra of four orthogonal subcarriers

Another way of thinking of this is that if one look at a matched receiver for one of the orthogonal functions, a subcarrier in the case of OFDM, then the receiver will only see the result for that function. The results from all other functions in the set integrate to zero, and thus have no effect.

$$\int_0^T S_i(t)S_j(t)dt = \begin{cases} C & i=j \\ 0 & i \neq j \end{cases} \tag{3.2}$$

Equation (3.3) shows a set of orthogonal sinusoids, which represent the subcarriers for an unmodulated real OFDM signal.

$$S_k(t) = \begin{cases} sin(2\pi k f_0 t) & 0 < t < T \quad k = 1, 2, ...M \\ 0 & otherwise \end{cases} \tag{3.3}$$

where f_0 is the carrier spacing, M is the number of carriers, T is the symbol period. Since the highest frequency componentis Mf_0, the transmission bandwidth is also Mf_0. These subcarriers are orthogonal to each other because when the waveforms of any two subcarriers are multiplied and integrate over the symbol period the result is zero. Multiplying the two sine waves together is the same as mixing these subcarriers. This results in sum and difference frequency components, which will always be integer subcarrier frequencies, as the frequency of the

two mixing subcarriers has integer number of cycles. Since the system is linear one can integrate the result by taking the integral of each frequency component separately then combining the results by adding the two sub-integrals. The two frequency components after the mixing have an integer number of cycles over the period and so the sub-integral of each component will be zero, as the integral of a sinusoid over an entire period is zero. Both the sub-integrals are zeros and so the resulting addition of the two will also be zero, thus it is established that the frequency components are orthogonal to each other.

3.2 OFDM Transmitter

In conventional OFDM system one transmitting antenna and one receiving antenna is used. Figure 3.3 shows the transmitter part of the OFDM system.

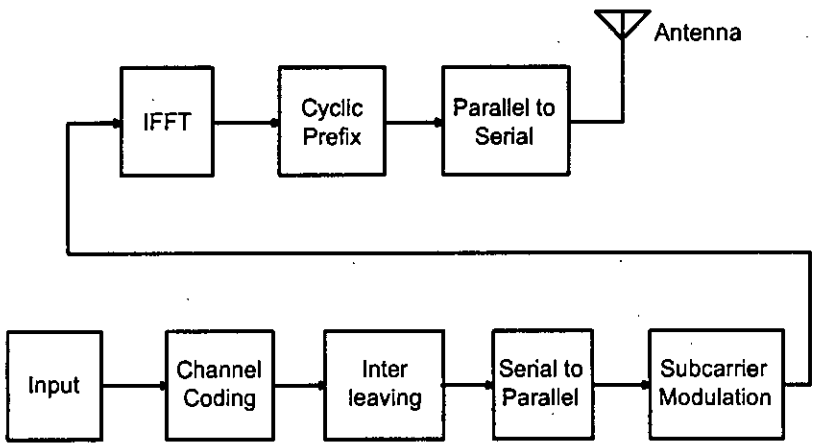

Figure 3.3: Block diagram of an OFDM transmitter

The transmitter section first converts digital data to coded data by coding and interleaving. The coded data is then transmitted by mapping of subcarrier amplitude and phase by subcarrier modulation technique. It then transforms this spectral representation of the data into the time domain using an inverse discrete fourier transform (IDFT). The inverse fast fourier transform (IFFT) performs the same operations as an IDFT, except that it is much more computationally efficient, and so is used in all practical systems. After IFFT, guard time is inserted to eliminate ISI and then it is converted back to serial form by serial to parallel conversion and then transmitted by the transmitting antenna.

3.2.1 Channel Coding

Since OFDM carriers are spread over a frequency range, there still may be some frequency selective attenuation on a time varying basis. A deep fade on a particular frequency may cause the loss of data on that frequency for that given time, thus some of the subcarriers can be strongly attenuated and that will cause burst errors. In these situations, forward error correction (FEC) in coded OFDM (COFDM) can fix the errors.

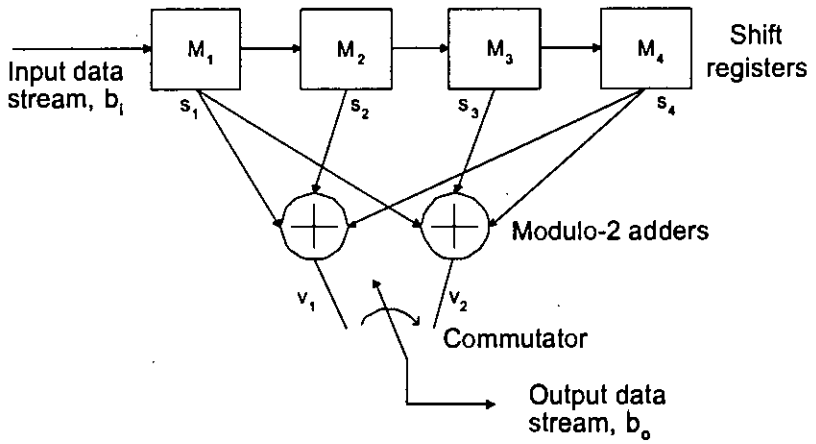

Figure 3.4: Convolutional encoder

An efficient FEC coding in flat fading situations leads to a very high coding gain, especially if soft decision decoding is applied. Thus, all OFDM systems now-a-days are converted to COFDM. The benefits of COFDM are two-fold in terms of performance improvement. First, the benefit that the channel coding brings in, is the robustness to burst error. Secondly, interleaving brings frequency diversity. The interleaver ensures that adjacent outputs from channel encoder are placed far apart in frequency domain.

A conventional encoder is illustrated in Figure 3.4. Here a convolutional code is generated by combining the outputs of a K-stage shift register (K=4) through the employment of v modulo-2 adders (v=2). Here M_1 through M_4 are 1-bit memory devices such as flip-flops. The outputs v_1 and v_2 of the modulo-2 adders in Figure 3.4 are

$$v_1 = s_1 \oplus s_2 \oplus s_4$$

$$v_2 = s_1 \oplus s_3 \oplus s_4$$

It is assumed that initially the shift register is clear. The first bit of the input data stream is entered into M_1. During the bit interval the commutator samples, in turn, the adder outputs v_1 and v_2. Thus a single bit yields, in the present case, two coded output bits. The encoder is therefore of rate 1/2. The next bit then enters M_1, while the bit initially in M_1 transfers to M_2, and the commutator again samples all the v adder outputs. This process continues until eventually the last bit of the input data has been entered into M_1. Thereafter, in order that every input bit may proceed entirely through the shift register, and hence be involved in the complete coding process, enough 0's are added to the message to transfer the last message bit through M_4, and, hence, out of the shift register. The shift register than finds itself in its initial "clear" condition.

From Figure 3.4, it is shown that for a single bit input, two output bits are present. So this types of encoder is 1/2 rate convolutional encoder. When this two bits are placed far apart from each other (i.e. placed on subcarriers that are far from each other in frequency domain), then they experience unique gain (and/or unique fade). It is very unlikely that both of the bits will face a deep fade, and thus at least one of the bits will be received intact on the receiver side, and as a result, overall performance will improve.

3.2.2 Interleaving

The OFDM subcarriers generally have different amplitudes because of the frequency selective nature of typical channels. Deep fades in the frequency spectrum may cause groups of subcarriers to be less reliable than others, thereby causing bit errors to occur in bursts rather than being randomly scattered. Most FEC codes are not designed to deal with burst errors. Therefore, interleaving is applied to randomize the occurrence of bit errors prior to decoding. At the transmitter, the coded bits are permuted in a certain way, which makes sure that adjacent bits are separated by several bits after interleaving. At the receiver, the reverse permutation is performed before decoding. A commonly used interleaving scheme is the block interleaver, where input bits are written in a matrix column by column and read out row by row.

Figure 3.5 shows the bit numbers of a block interleaver operating on a block size of 35 bits. After writing the 35 bits in the matrix according to the order as depicted in the Figure 3.5, the interleaved bits are read out row by row, so

0	7	14	21	28
1	8	15	22	29
2	9	16	23	30
3	10	17	24	31
4	11	18	25	32
5	12	19	26	33
6	13	20	27	34

Figure 3.5: Interleaving scheme

the output bit numbers are 0,7,14,..., . Instead of bits, the operation can also be applied on symbols; for instance, the matrix can be filled with 35 16 – QAM symbols containing 4 bits per symbol, so the interleaving changes the symbol order but not the bit order within each symbol.

3.2.3 Serial to Parallel Conversion

Normally data is transmitted in the form of a serial data stream. In OFDM, each symbol typically transmits multiple bits, and so a serial to parallel conversion stage is needed to convert the input serial bit stream to the data to be transmitted in each OFDM symbol. The data allocated to each symbol depends on the modulation scheme used and the number of subcarriers. For example, for a subcarrier modulation of 16-QAM each subcarrier carries 4 bits of data, and so for a transmitter using 200 subcarriers the number of bits per symbol would be 800.

For adaptive modulation schemes, the modulation scheme used on each subcarrier can vary and so the number of bits per subcarrier. As a result the serial to parallel conversion stage involves filling the data payload for each subcarrier. At the receiver the reverse process takes place, with the data from the subcarriers being converted back to the original serial data stream.

3.2.4 Subcarrier Modulation

Once each subcarrier has been allocated bits for transmission, they are mapped using a modulation scheme to a subcarrier amplitude and phase, which is represented by a complex In-phase and Quadrature-phase (IQ) vector. Figure 3.6 shows an example of subcarrier modulation mapping.

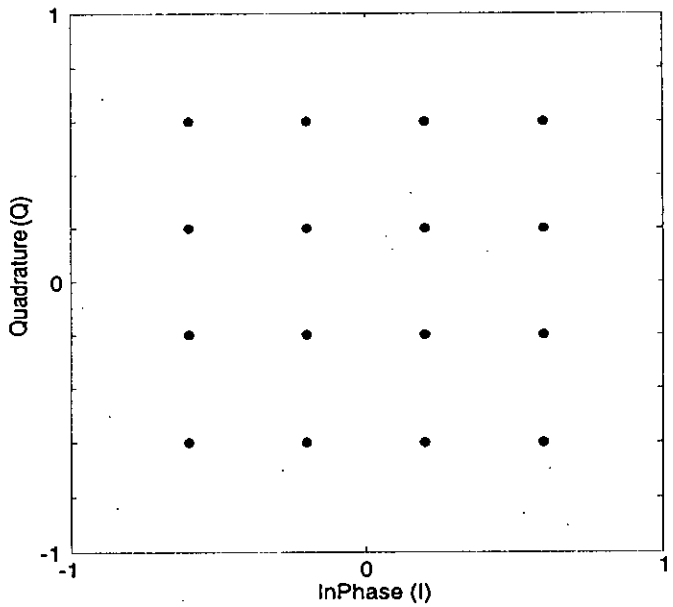

Figure 3.6: Example IQ modulation constellation. 16-QAM

This example shows 16-QAM, which maps 4 bits for each symbol. Each combination of the 4 bits of data corresponds to a unique IQ vector, shown as a dot on Figure 3.6. A large number of modulation schemes are available allowing the number of bits transmitted per carrier per symbol to be varied.

Imaginary Subcarrier modulation can be implemented using a lookup table, making it very efficient to implement. In the receiver, mapping the received IQ vector back to the data word performs subcarrier demodulation. During transmission, noise and distortion becomes added to the signal due to thermal noise, signal power reduction and imperfect channel equalization. Figure 3.7 shows an example of a received 16-QAM signal. Each of the IQ points is blurred in location due to the channel noise.

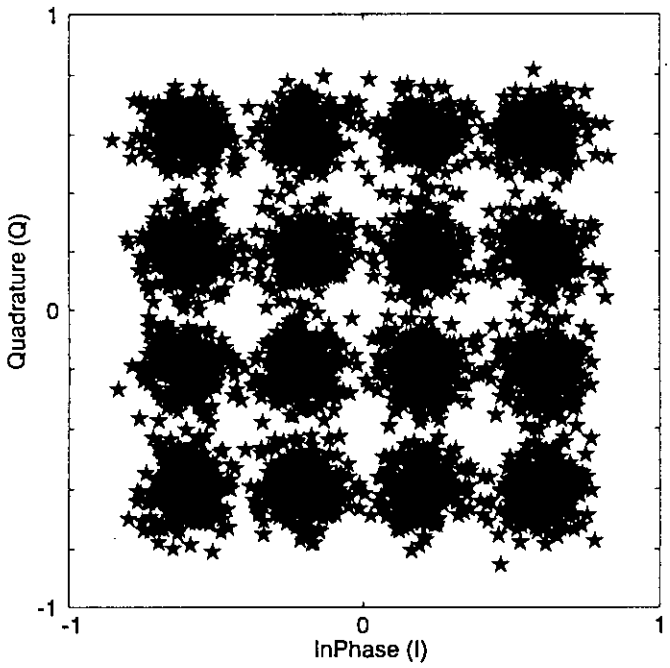

Figure 3.7: Example IQ demodulation constellation. 16-QAM

3.2.5 Inverse Fast Fourier Transform

After the subcarrier modulation stage each of the data subcarriers is set to an amplitude and phase based on the data being sent and the modulation scheme; all unused subcarriers are set to zero. This sets up the OFDM signal in the frequency domain. An IFFT is then used to convert this signal to the time domain, allowing it to be transmitted. Figure 3.8 shows the IFFT section of the OFDM. In the frequency domain, before applying the IFFT, each of the discrete samples of the IFFT corresponds to an individual subcarrier. Most of the subcarriers are modulated with data. The other subcarriers are unmodulated and set to zero amplitude. These zero subcarriers provide a frequency guard band before the Nyquist frequency and effectively act as an interpolation of the signal and allows for a realistic roll off in the analog anti-aliasing reconstruction filters.

3.2.6 Cyclic Prefix

For a given system bandwidth the symbol rate for an OFDM signal is much lower than a single carrier transmission scheme. For example for a single carrier binary phase shift keying (BPSK) modulation, the symbol rate corresponds to the bit

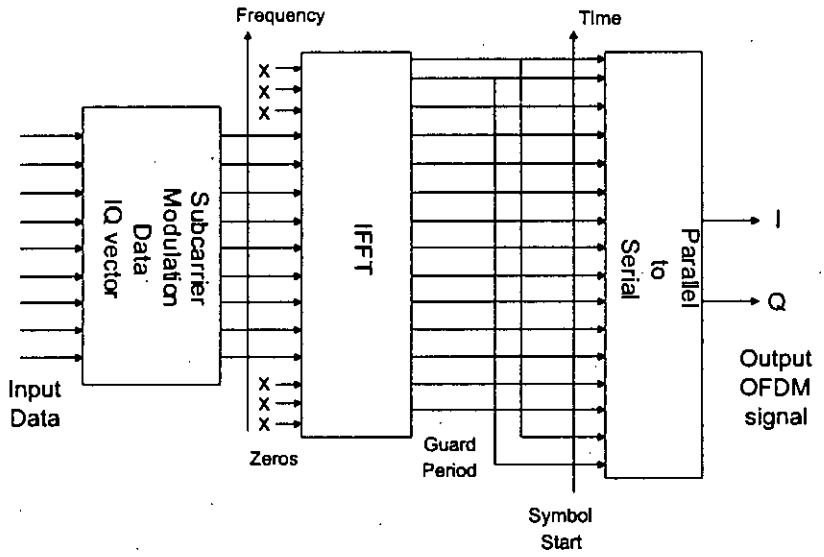

Figure 3.8: OFDM generation at IFFT stage

rate of the transmission. However for OFDM the system bandwidth is broken up into N_c subcarriers, resulting in a symbol rate that is N_c times lower than the single carrier transmission. This low symbol rate makes OFDM naturally resistant to effects of ISI caused by multipath propagation. In an OFDM system, it also makes that the orthogonality of the subcarriers is lost, resulting in ICI.

To overcome these problems, Peled and Ruiz [33] introduced the Cyclic Prefix (CP). A cyclic prefix is a copy of the last part of the OFDM symbol that is added to the transmitted symbol and removed at the receiver before the demodulation. The cyclic prefix should be at least as long as the significant part of the impulse response experienced by the transmitted signal. This way the benefit of the cyclic prefix is twofold. First, it avoids the ISI because it acts as a guard space between successive symbols. Second, it also converts the linear convolution with the channel impulse response into a cyclic convolution. As a cyclic convolution in the time domain translates into a scalar multiplication in the frequency domain, the subcarriers remain orthogonal and there is no ICI. Figure 3.9 shows the insertion of a guard period.

The length of the cyclic prefix should be made longer than the experienced impulse response to avoid ISI and ICI. However, the transmitted energy increases with the length of the cyclic prefix. The SNR loss due to the insertion of the CP

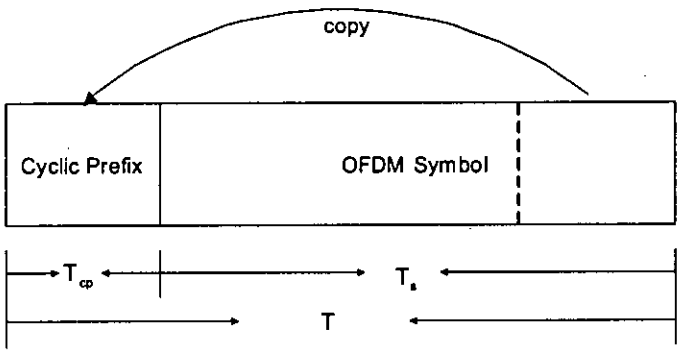

Figure 3.9: Insertion of guard time

is given by

$$SNR_{loss} = -10log_{10}(1 - \frac{T_{cp}}{T}) \tag{3.4}$$

Where T_{cp} denotes the length of the cyclic prefix and $T = T_{cp} + T_s$ is the length of the transmitted symbol. Because of the loss of SNR and efficiency, the cyclic prefix should not be made longer than strictly necessary.

3.2.7 Parallel to Serial Conversion

After cyclic prefix is added to the OFDM system, a parallel to serial conversion is taken place. So after parallel to serial conversion data is transmitted in the form of a serial data stream.

3.3 OFDM Receiver

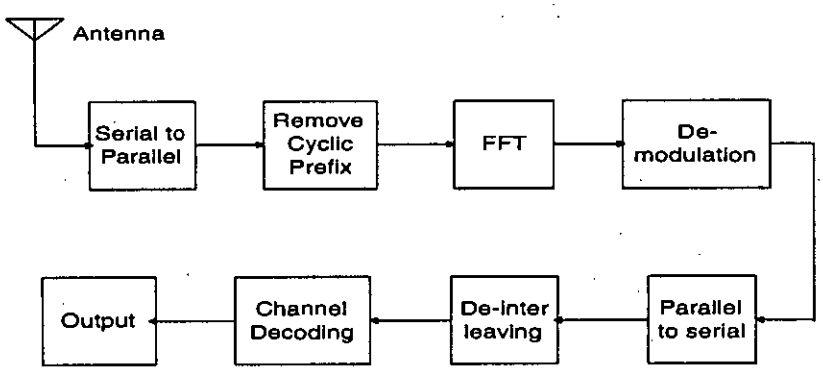

Figure 3.10: Block diagram of an OFDM receiver with single antenna

The receiver performs the reverse operation of the transmitter. Received data is first transformed into parallel data stream. After that cyclic prefix is removed and using Fast Fourier Transform (FFT) the signal is backed in the frequency domain. The amplitude and phase of the subcarriers are then picked out by demodulation of quadrature amplitude modulation and converted back to digital data. This digital data is then decoded by Viterbi decoder to get the received data. Fig. 3.10 shows the receiver part of the OFDM system.

3.4 Implementation Complexity of OFDM Versus Single-Carrier Modulation

One of the main reasons to use OFDM is its ability to deal with large delay spreads with a reasonable implementation complexity. Many researcher have investigated the performance of OFDM over a single-carrier modulation scheme [34]-[36]. It is well known that OFDM is more effective to combat ISI compared with a single-carrier system using a time-domain equalizer, especially for channels with large delay spread. Moreover, the efficiency of FFT algorithms implemented in OFDM also makes the computational complexity much less than the time-domain equalization in a single - carrier system [37]. However, for large FFT sizes, a single -carrier system employing frequency domain equalization has much lower complexity as compared with time-domain equalization [38]. Recent papers usually compare the system performance of an OFDM system with a single-carrier system employing frequency-domain equalization because the complexities are comparable.

Two main issues come up from the comparison of an OFDM system with a single-carrier system. The first one is the power amplification issue. If the data sequence is modulated using phase shift keying (PSK) scheme, then the output signal has a low envelope fluctuation with a compact spectrum for a single-carrier system. For a multi-carrier system, such as OFDM, the envelope fluctuation is large. In fact, according to the central limit theorem, the real and imagery parts of an OFDM symbol are Gaussian distributed for a large number of subcarriers, making the envelope of the OFDM signal Raleigh distributed. A signal with large envelope fluctuation requires a power amplifier with large backoff, which makes the amplifier power inefficient. Therefore, the power amplifier for a single-carrier

system has a good power efficiency compared with that for an OFDM system.

The second issue is the impact of the channel coding to system performance. The performance of a communication system is usually measured in terms of BER for a specific SNR. Consider the case in which the channel is frequency-selective. For a single -carrier system using the frequency domain equalization scheme, once the channel is equalized in the frequency domain, the signal is converted back to the time domain before decision is made on individual bits. This means that the energy of an individual bit is distributed over the entire frequency spectrum. On the other hand, since the decision-making process is performed in the frequency domain for an OFDM system, the energy of an individual bit occupies only a small portion of the entire frequency spectrum. As a result, a deep notch at a certain frequency range over the channel bandwidth decreases the bit energy slightly for a single-carrier system, but for OFDM it may significantly attenuate the bit energy across several subcarriers, making the bits on those subcarriers unreliable. In fact, the BER for a single-carrier system is dominated by the average SNR over the entire channel bandwidth, while for an OFDM system it is dominated by the subcarriers with the smallest SNR. To reduce the BER of OFDM caused by frequency-selective fading, one can set to zero those subcarriers (referred to as virtual subcarriers) that experience deep notches before performing IFFT on the transmitter side. However, if the channel is time-varying, deep notches will appear randomly across the channel bandwidth. In this case, channel coding with error correction capability is needed to make the bits on those deep notches more reliable and reduce the BER.

A block code [39] with code length equal to the FFT block length together with hard-decision decoding is a good choice as long as the code can correct the errors per block with a high probability. Reed-Solomon codes [40] are the most widely used block codes due to their good distance properties and efficiency in coding and decoding. A better strategy is to use a convolutional code with interleaving in the frequency domain and soft-decision decoding. Since convolutional coding is not effective to correct burst errors and deep notches usually affect a contiguous group of subcarriers, frequency-domain interleaving provides frequency diversity and making convolutional coding more effective to combat frequency-selective fading.

3.5 Summary

This chapter begins with the basic concept of multicarrier modulation and orthogonality which are the main concepts of the OFDM. After that, the detail block diagrams of the OFDM transmitter (i.e. forward error correction coding, interleaving, subcarrier modulation, FFT and guard time) and receiver are depicted. Finally,th e implementation complexity between the OFDM and the single carrier communication systems is explained.

Chapter 4

Smart Antennas with OFDM

In this chapter a smart antenna based OFDM system is proposed. In the proposed model a single antenna is used at the transmitter end and multiple antennas are used at the receiver end. This proposed system is called single input and multiple output (SIMO) in the literature. An analytical formulation of the BER, channel capacity and throughput for the proposed system is also presented in this chapter.

4.1 Proposed OFDM Receiver

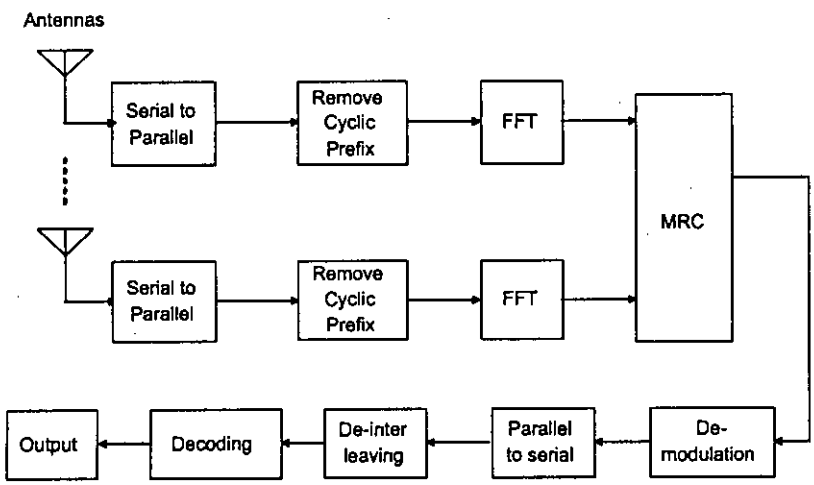

Figure 4.1: Block diagram of a conventional OFDM receiver with multiple antennas

In the proposed smart antenna based OFDM system, only one antenna is used at the transmitter side and multiple antennas are used at the receiver side. So

at the transmitter side, the proposed system is just like any conventional OFDM transmitter. In the chapter 3, the transmitter part of the OFDM system is discussed extensively. At the receiver part the proposed system is different, here an OFDM system with multiple receiving antennas are used. Signals received by the multiple antennas are combined by the maximum ratio combining method and this combining signals are processed at the receiver.

In a conventional multiple antenna based receiver, each FFT processing corresponds to one receiver antenna. Figure 4.1 shows the diagram of that receiver. Here, After the FFT processing, subcarrier based space combining is employed. However, the complexity is huge because multiple FFT processing is needed for each OFDM symbol.

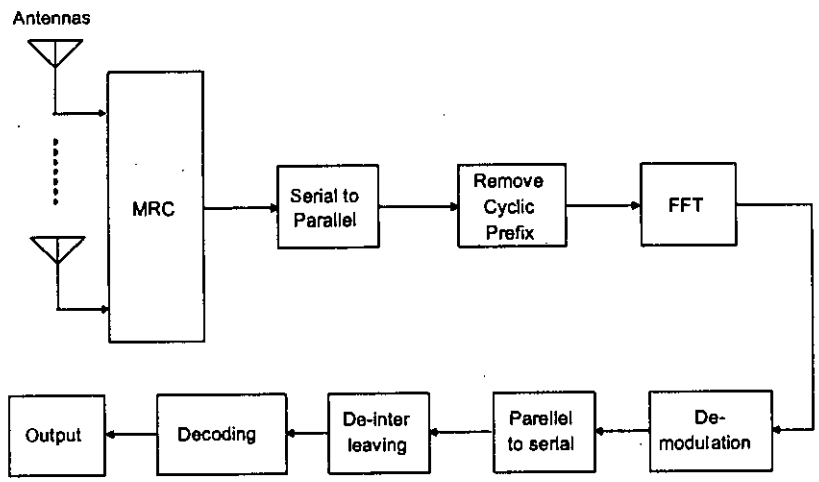

Figure 4.2: Block diagram of the proposed OFDM receiver with multiple antennas

To reduce the number of FFT processing required for each OFDM symbol, a general receiver architecture is shown in figure 4.2. In the proposed architecture, a group of K received OFDM symbols with M replicas (each replica corresponds to the output of one antenna attenuated by the corresponding channel) are firstly processed by the pre-FFT processing block, i.e. the maximum ratio combing block, in the time domain. After that, signals are processed by FFT processor. As the combining operations are performed at the subcarrier level before the FFT operation, this process is known as Pre-FFT MRC. The computational complexity of the proposed system is less as only one FFT processor is needed for the system. After that the FFT processed signals are processed just like any

conventional receiver.

4.2 OFDM System Model

The discrete-time baseband equivalent model of the proposed OFDM transmitter is given in figure 4.3.

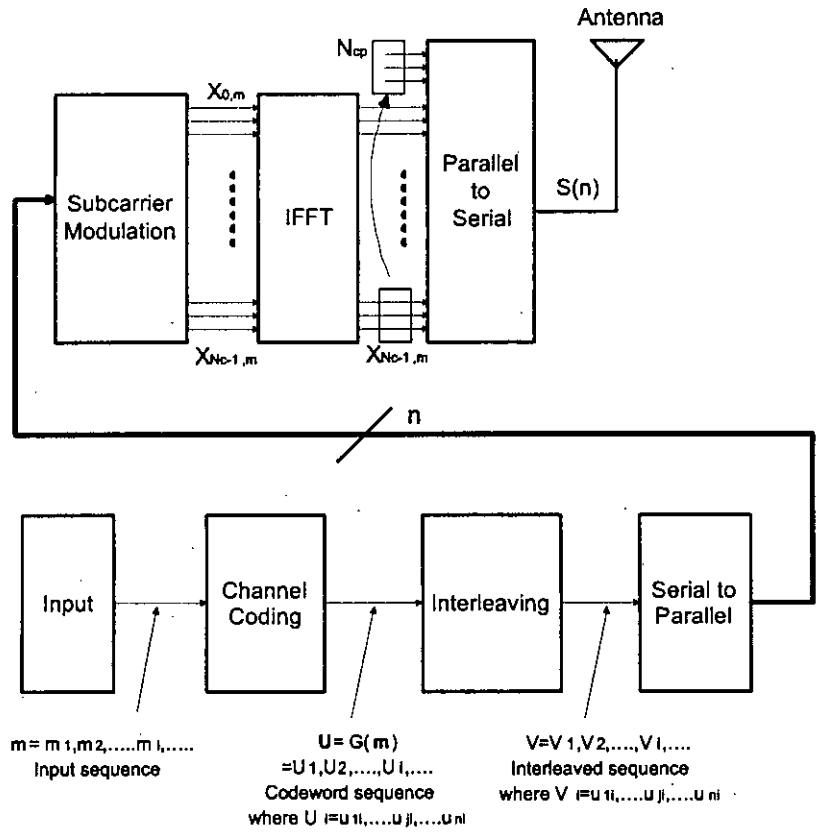

Figure 4.3: Discrete time baseband equivalent model of an OFDM transmitter

In the transmitter, the input data is denoted by the sequence $\mathbf{m} = m_1, ..., m_i$, where each m_i represents a binary digit (bit), and i is a time index. It is assumed that each m_i equally likely to be a one or a zero, and independent from digit to digit. The convolutional coder transforms each sequence $\mathbf{m}$ into a unique codeword sequence $\mathbf{U} = G(\mathbf{m})$. The sequence $\mathbf{U}$ can be partitioned into a sequence of branch words: $\mathbf{U} = U_1, U_2, ..., U_i, ...$ Each branch word U_i is made up of binary code symbols, often called channel symbols; unlike the input data the code symbols are not independent. The code sequence $\mathbf{U}$ is transformed to

V by interleaver. After that incoming data stream is grouped in blocks of N_c data symbols. These groups are called OFDM symbols and can be represented by a vector $\mathbf{x}_m = (x_{0,m} \quad x_{1,m} \quad ..... \quad x_{N_c-1,m})^T$. Next, an IFFT is performed on each data symbol block, and a cyclic prefix of length N_{cp} is added. The resulting complex baseband discrete time signal of the m^{th} OFDM-symbol can be written as

$$s_m(n) = \begin{cases} \frac{1}{N_c} \sum_{k=0}^{N_c-1} x_{k,m} e^{j2\pi k(n-N_{cp})/N_c} & \text{if } n \in [0, N_c + N_{cp} - 1] \\ 0 & \text{otherwise} \end{cases} \tag{4.1}$$

where n is the discrete time index.

The complete time signal $s(n)$ is given by the concatenation of all OFDM symbols that are transmitted

$$s(n) = \sum_{m=0}^{\infty} s_m(n - m(N_c + N_{cp})) \tag{4.2}$$

The discrete-time baseband equivalent model of the proposed OFDM receiver is given in figure 4.4.

In general received signal is the sum of a linear convolution with the discrete channel impulse response $h(n)$ and additive white Gaussian noise $n(n)$. For this, one implicitly assume that the channel fading is slow enough to consider it constant during one OFDM symbol. In addition, it is assumed that the transmitter and receiver are perfectly synchronized. Based on the fact that the cyclic prefix is sufficiently long to accommodate the channel impulse response, or $h(n) = 0$ for $n < 0$ and $n > N_{cp} - 1$, for jth receiver, it can be written:

$$r_j(n) = \sum_{\eta=0}^{N_{cp}} h_j(\eta) s(n - \eta) + n_j(n) \tag{4.3}$$

If the gain of the 1^{st} antenna is γ_1, 2^{nd} antenna is γ_2, ... J^{th} antenna is γ_J, then the received signal of each antenna is according to MRC and the output is

$$r(n) = \frac{r_1(n) \times \gamma_1^*}{\gamma_1^2 + \gamma_2^2 ..... + \gamma_J^2} + \frac{r_2(n) \times \gamma_2^*}{\gamma_1^2 + \gamma_2^2 ..... + \gamma_J^2} + ... + \frac{r_j(n) \times \gamma_J^*}{\gamma_1^2 + \gamma_2^2 ..... + \gamma_J^2} \tag{4.4}$$

Now the received signal $r(n)$ is split into blocks and the cyclic prefix associated with each block is removed. This results in a vector $\mathbf{r}_m = (r(z_m) \quad r(z_m + 1) \quad ..... \quad r(z_m + N_c - 1)^T$, with $z_m = m(N_c + N_{cp}) + N_{cp}$. The received data

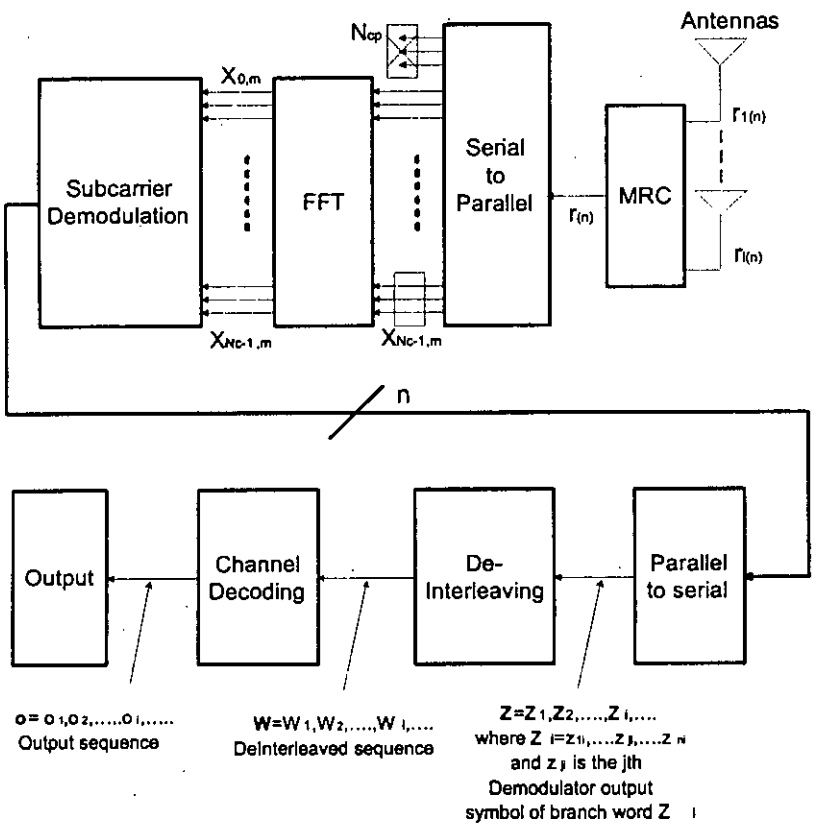

Figure 4.4: Discrete time baseband equivalent model of an OFDM receiver

symbol $y_{k,m}$ is obtained by performing a N_c-point FFT on this vector. Thus $y_{k,m}$ is given by

$$y_{k,m} = \sum_{n=0}^{N_c-1} r(z_m + n)e^{-j2\pi kn/N_c} \tag{4.5}$$

by substituting $r(n)$ with Equation (4.3),(4.5) can be written as

$$y_{k,m} = \sum_{n=0}^{N_c-1}(\sum_{\eta=0}^{N_{cp}-1} h(\eta)s_m(N_{cp}+n-\eta))e^{j2\pi kn/N_c} + \sum_{n=0}^{N_c-1} n(z_m+n)e^{j2\pi kn/N_c} \tag{4.6}$$

substituting $s_m(n)$ with Equation (4.1), then yields the following result:

$$y_{k,m} = \sum_{n=0}^{N_c-1}(\sum_{\eta=0}^{N_{cp}-1} h(\eta)\frac{1}{N_c}\sum_{k=0}^{N_c-1} x_{k,m}e^{j2\pi k(n-\eta)/N_c})e^{-j2\pi kn/N_c} + n_{k,m} \tag{4.7}$$

where $n_{k,m} = \sum_{n=0}^{N_{cp}-1} n(z_m+n)e^{-j2\pi kn/N_c}$ is the k^{th} sample of the N_c point FFT of $n(z_m+n)$. since $n(n)$ is white Gaussian noise, $n_{k,m}$ is also white Gaussian noise.

Because $h(\eta) = 0$, for all $\eta > Ncp - 1$, one can let η run from 0 to $N_c - 1$ instead of $N_{cp} - 1$. Additional swapping of the two inner sums and reordering yields

$$y_{k,m} = \underbrace{\sum_{n=0}^{N_c-1} \underbrace{(\frac{1}{N_c} \sum_{k=0}^{N_c-1} (\sum_{\eta=0}^{N_c-1} h(\eta) e^{-j2\pi kn/N_c}) x_{k,m} e^{j2\pi kn/N_c})}_{IFFT} e^{-j2\pi kn/N_c}}_{FFT} + n_{k,m} \quad (4.8)$$

The first part of this expression consists of an IFFT operation nested in a FFT operation. The inner sum is the k^{th} sample of the N_c-point FFT of $h(n)$, of h_k. The equation hence translates into

$$y_{k,m} = h_k x_{k,m} + n_{k,m} \quad (4.9)$$

This equation demonstrates that the received data symbol $y_{k,m}$ on each subcarrier k equals the data symbol $x_{k,m}$ that was transmitted on that subcarrier, multiplied by the corresponding frequency domain channel coefficient h_k in addition to the transformed noise contribution $n_{k,m}$.

Now the received data symbol is demodulated to $\mathbf{Z} = Z_1, Z_2, ..., Z_i$ as indicated in Figure 4.4. The task of the Veterbi decoder is to produce as output bit sequence $\mathbf{o} = o_1, o_2, ..., o_i, ...$

4.3 Analytical formulation of Bit Error Rate

In an OFDM system, the received data symbol transmitted in the m^{th} signalling interval on the k^{th} subcarrier is given by the corresponding transmitted symbol, multiplied with the channel frequency response sampled at the k^{th} subcarrier frequency h_k plus noise. If it has an ideal linear time-invariant (LTI) frequency non-dispersive additive white Gaussian noise (AWGN) channel, this translates to a parallel set of AWGN channels, with equal SNR. As a consequence, the performance will be identical with single carrier modulation over AWGN, except for the SNR loss due to the cyclic prefix.

As the proposed modulation scheme for OFDM is QAM, it has to calculate the BER of QAM. A block diagram for a generic inphase quadrature phase modulator is found in figure 4.5. It is shown that the transmitted signal can be viewed as the sum of two PAM processes with different pulse shapes $\Psi I(t)$ in the top (in

phase) branch and $\Psi_Q(t)$ in the lower (quadrature) branch where,

$$\Psi_I = \sqrt{\frac{2}{E_g} g_T(t) cos(2\pi f_c t)} \tag{4.10}$$

$$\Psi_Q = \sqrt{\frac{2}{E_g} g_T(t) sin(2\pi f_c t)} \tag{4.11}$$

Here, E_g is the energy of the pulse shape$g_T(t)$. The general case when both amplitude and phase is allowed to change between signal alternatives is called quadrature amplitude modulation (QAM). There are many possible QAM constellations but here only square constellation (4-QAM, 16-QAM, 64-QAM) is considered. Constellation sizes such that $M = 2^k$, where k is an integer. As seen in the figure 4.6, the signal vectors are spaced with the distance $2A$ along the axes (the value of A is arbitrary). Hence the minimum distance of the constellation is $d_{min} = 2A$.

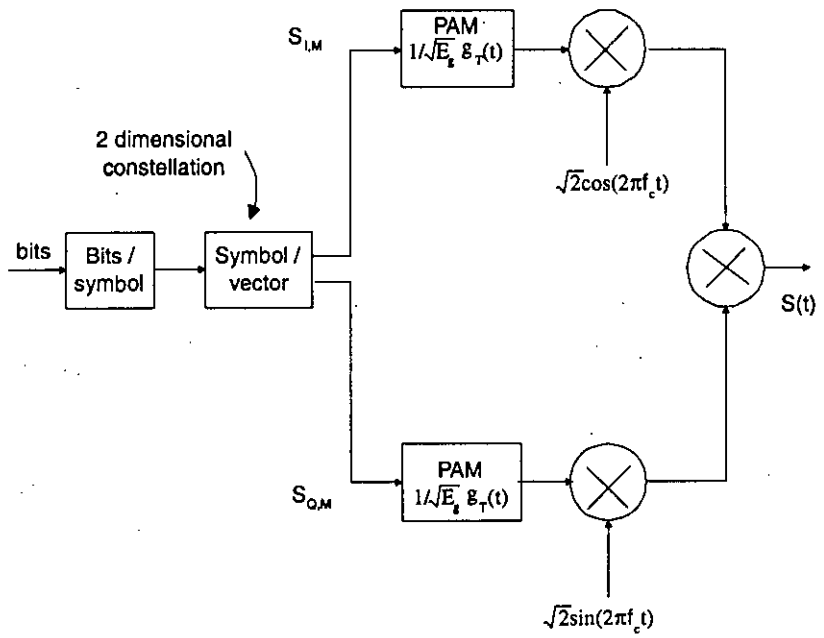

Figure 4.5: Generic IQ Modulation

When M is an even square, there will be $\sqrt{M}$ possible amplitude for both s_I and s_Q. Infect,

$$s_I \in \{\pm A, \pm 3A, \pm 5A, ..., \pm A(\sqrt{M}-1)\}$$

$$s_Q \in \{\pm A, \pm 3A, \pm 5A, ..., \pm A(\sqrt{M}-1)\}$$

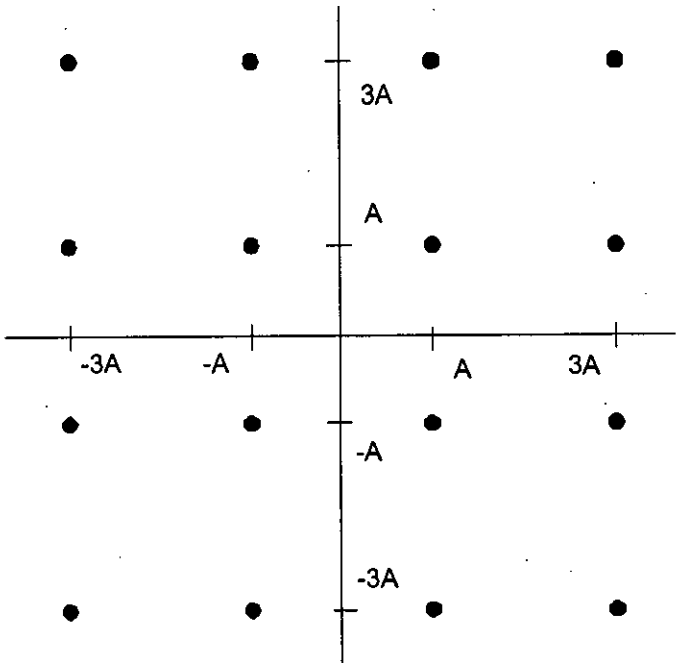

Figure 4.6: Rectangular QAM constellation

Regardless of M is an even square or not, the maximum likelihood (ML) decision region will be rectangular shaped. The regions can be squares (type I), squares with one open side (type II), or square with two open sides (type III). Figure 4.7 shows the diagram. For a 16-QAM has, [4] points who have type I, [8] points who have type II, [4] points who have type III. In general for a M-ary QAM has, $[(\sqrt{M}-2)^2]$ points who have type I,$[M-(\sqrt{M}-2)^2-4]$ points who have type II, [4] points who have type III. So, on the average a point have closest point:

$$\begin{aligned} &= \frac{1}{M}[(M-4\sqrt{M}+4)\times 4+(4\sqrt{M}-8)\times 3+4\times 2] \\ &= 4(1-\frac{1}{\sqrt{M}}) \end{aligned}$$

Now all the closest points are equal distance apart and this distance is $[\sqrt{E_{min}}-(-\sqrt{E_{min}})]$ or $2\sqrt{E_{min}}$, where E_{min} is the energy of the signal with lowest amplitude. For a 16-QAM with signal constellation as shown in figure 4.8, the L by L, where $L=\sqrt{M}$ matrix is

$$\begin{pmatrix} (-3,3) & (-1,3) & (1,3) & (3,3) \\ (-3,1) & (-1,1) & (1,1) & (3,1) \\ (-3,-1) & (-1,-1) & (1,-1) & (3,-1) \\ (-3,-3) & (-1,-3) & (1,-3) & (3,-3) \end{pmatrix}$$

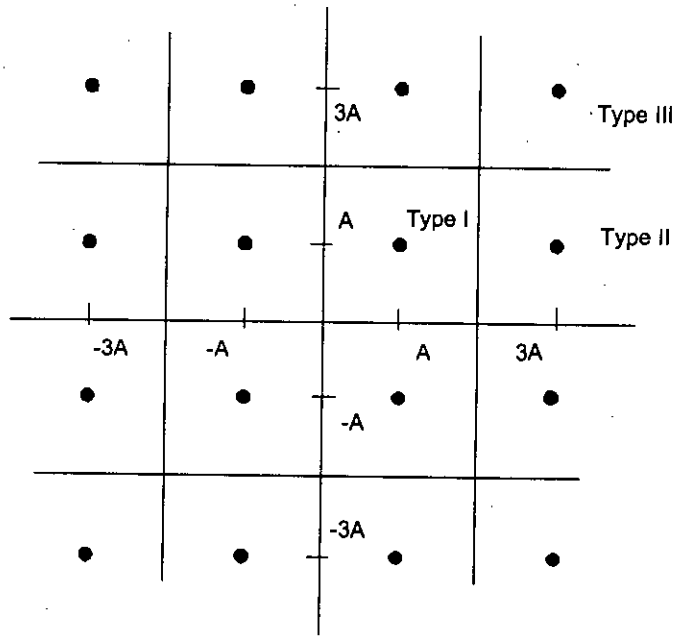

Figure 4.7: ML decision region for 16-QAM

So the average energy of the signal is

$$\begin{aligned} E_{avg} &= \frac{1}{M}\sum(x^2+y^2)(\sqrt{E_{min}})^2 \\ &= \frac{E_{min}}{M}\sum(x^2+y^2) \end{aligned} \tag{4.12}$$

from the $16-QAM$ matrix it is shown that here 4 or $\sqrt{16}$ or $\sqrt{M}$ no of -3,3,-1,1

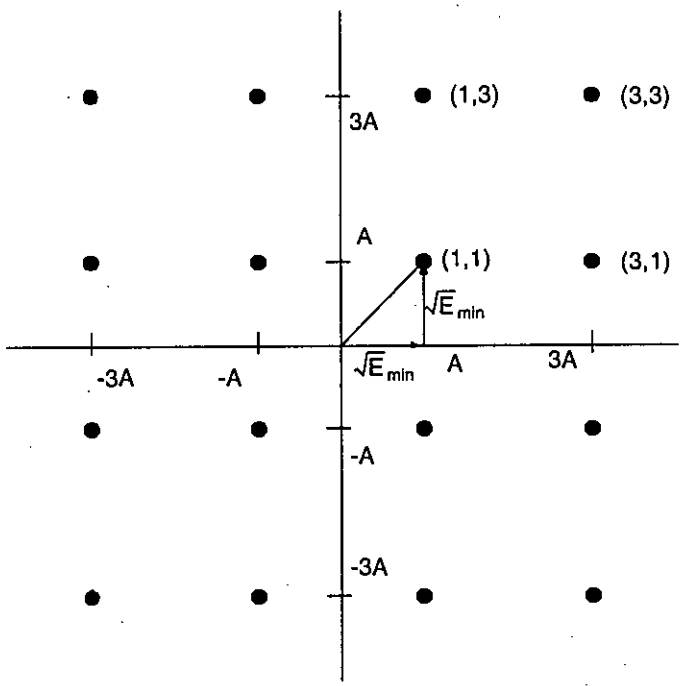

Figure 4.8: 16-QAM with signal constellation

for x and y axis. So

$$\begin{aligned}
E_{avg} &= \frac{E_{min}}{M}(\sqrt{M}\sum x^2 + \sqrt{M}\sum y^2) \\
&= \frac{E_{min}}{\sqrt{M}}(\sum x^2 + \sum y^2) \\
&= \frac{E_{min}}{\sqrt{M}} 2\sum x^2 \\
&= \frac{2E_{min}}{\sqrt{M}}[2(1^2 + 3^2 + ... + (\sqrt{M}-1)^2] \\
&= \frac{4E_{min}}{\sqrt{M}}\frac{(\sqrt{M}-1)(\sqrt{M}-1+1)(\sqrt{M}-1+2)}{6} \\
&= \frac{2E_{min}}{\sqrt{M}}\frac{(\sqrt{M}-1)(\sqrt{M}+1)(\sqrt{M})}{3} \\
&= 2E_{min}\frac{M-1}{3} \\
E_{min} &= \frac{3E_{avg}}{2(M-1)} \qquad (4.13)
\end{aligned}$$

Now, the distance between 2 closest points is $2\sqrt{E_{min}}$ and in average there are $4(1-\frac{1}{\sqrt{M}})$ closest points around a point. So the average probability of bit error

is,

$$P_e = 4(1-\frac{1}{\sqrt{M}})Q(\frac{2\sqrt{E_{min}}}{\sqrt{2N_0}}) = 4(1-\frac{1}{\sqrt{M}})Q(\sqrt{\frac{2E_{min}}{N_0}}) \quad (4.14)$$

putting the value of E_{min} in Equation (4.13) one get,

$$P_e = 4(1-\frac{1}{\sqrt{M}})Q(\sqrt{\frac{3E_{avg}}{(M-1)N_0}}) \quad (4.15)$$

So, the average symbol error probability in an AWGN channel for M-ary QAM, using coherent detection can be approximated by

$$P_e = 4(1-\frac{1}{\sqrt{M}})Q(\sqrt{\frac{3E_{avg}}{(M-1)N_0}}) \quad (4.16)$$

where E_{avg}/N_0 is the average SNR per symbol. To obtain bit error probability from the symbol error probability, it can observed that square QAM can be perfectly Gray coded. That is, there is only one bit difference between adjacent symbols. Each symbol error must likely causes one bit error at large SNR. Thus

$$P_b \cong \frac{P_e}{log_2 M} = \frac{4(\sqrt{M}-1)}{\sqrt{M}log_2 M}Q(\sqrt{\frac{3E_{avg}}{(M-1)N_0}}) \quad (4.17)$$

since the average energy per bit is, $E_b = E_{avg}/log_2 M$, Equation (4.17) can be written as

$$P_b = \frac{4(\sqrt{M}-1)}{\sqrt{M}log_2 M}Q(\sqrt{(\frac{3log_2\sqrt{M}}{M-1})\frac{2E_b}{N_0}}) \quad (4.18)$$

or,

$$P_b = \frac{2(L-1)}{Llog_2 L}Q(\sqrt{(\frac{3log_2 L}{L^2-1})\frac{2E_b}{N_0}}) \quad (4.19)$$

4.3.1 BER for Flat Fading Channel

In a flat fading channel, the signal undergoes a multiplicative variation. In general this multiplicative factor is complex, that is, the signal amplitude as well as phase are affected. If it further assume that the fading is slow, then the amplitude attenuation and phase shift of the received signal can be considered constant

over at least a symbol duration. Therefore, if the transmitted equivalent low-pass complex signal is $\tilde{s}(t)$, the received signal can be written as

$$\tilde{r}(t) = ze^{-j\phi}\tilde{s}(t) + \tilde{n}(t) \tag{4.20}$$

where z is the amplitude of the signal, ϕ is the phase shift of the signal caused by the channel, and $\tilde{n}(t)$ is the additive Gaussian noise.

Now, the average error probability can be evaluated by averaging the error probability for a fixed amplitude z over the entire range of z. that is

$$P_e = \int_0^\infty p_e(\gamma_b)p(\gamma_b)d\gamma_b \tag{4.21}$$

where

$$\gamma_b = z^2 E_b/N_0$$

is the signal-to-noise ratio with fading for a particular value of z, $P_e(\gamma_b)$ is the symbol or bit error probability conditioned on a fixed γ_b and $p(\gamma_b)$ is the probability density function of γ_b and p_e is the average symbol or bit error probability.

4.3.2 BER for Rayleigh Fading Channel

For Rayleigh fading channel, z has a Rayleigh distribution, thus z^2 and γ_b have a chi-square distribution with two degree of freedom. That is

$$p(\gamma_b) = \frac{1}{\tau}exp(-\frac{\gamma_b}{\tau}); \quad \tau \geq 0 \tag{4.22}$$

where,

$$\tau = E\{z^2\}\frac{E_b}{N_0}$$

is the average value of the signal-to-noise ratio.

Substituting the error probability expression of QAM modulation in the AWGN channel and Equation (4.22) into Equation (4.21), one can obtain the error probability expression of the modulation in a slow, Rayleigh fading channel.

For QAM modulation scheme, the symbol or bit error rate in the AWGN channel can be expressed as

$$\begin{aligned} P_b &= \frac{2(L-1)}{Llog_2L}Q(\sqrt{(\frac{3log_2L}{L^2-1})\frac{2E_b}{N_0}}) \\ &= CQ(\sqrt{\frac{\delta E_b}{N_0}}) \end{aligned}$$

where C and δ are constant, and their value is

$$C = \frac{2(L-1)}{Llog_2 L}$$
$$\delta = \frac{6log_2 L}{L^2-1}$$

In the fading channel, the signal-to-noise ratio E_b/N_0 becomes $\gamma_b = z^2 E_b/N_0$. Correspondingly the conditional error probabilities are

$$P_b(\gamma_b) = CQ(\sqrt{\delta\gamma_b}) \tag{4.23}$$

Substituting Equation (4.23) into Equation (4.21), one can obtain the corresponding bit error probabilities.

For the Q function $P_e(\gamma_b)$ is evaluated using the following two formulas. The first is

$$\int_0^\infty [1 - erf(\beta x)]e^{-\mu x^2} = \frac{1}{2\mu}(1 - \frac{\beta}{\sqrt{\mu+\beta^2}}) \tag{4.24}$$

and the second is the well-known relation between the error function and the Q function

$$1 - erf(x) = 2Q(\sqrt{2}x) \tag{4.25}$$

which is used to convert the Q function into the error function in order to use Equation (4.24). Substituting Equation (4.23) and Equation (4.22) into Equation (4.21), and making a variable change $\gamma_b = x^2$, one have

$$P_s = \int_0^\infty \frac{C}{\tau}[1 - erf(\sqrt{\frac{\delta}{2}}x)]e^{-\frac{x^2}{\tau}}xdx \tag{4.26}$$

Recognizing $\sqrt{\delta 2} = \beta$ and $1/\tau = \mu$ in Equation (4.24), the above is equal to

$$P_s = \frac{C}{2}[1 - \sqrt{\frac{\delta\tau}{2+\delta\tau}}] \tag{4.27}$$

4.3.3 BER for Frequency Selective Fading Channel

In a frequency selective fading channel, the received signal contains multiple delayed versions of the transmitted signal. The multipath signals cause intersymbol interference which results in an irreducible BER floor. The BER falls initially with the increase of the signal-to-noise ratio (E_b/N_o), and stops falling when the signal-to-noise ratio is sufficiently high at which the errors floor, it is clear that the BER floor is directly related to the delays of the multipath components. Simulation is the main tool of studying BER behavior in frequency selective channel in OFDM.

4.4 Analytical formulation of Channel Capacity

If OFDM system consists of nT transmitter and nR receiver antenna then channel is defined by an $nR \times nT$ complex matrix (denoted by symbol H) shown in Figure 4.9. The transmitted signal is represented by an $nT \times 1$ column matrix (denoted

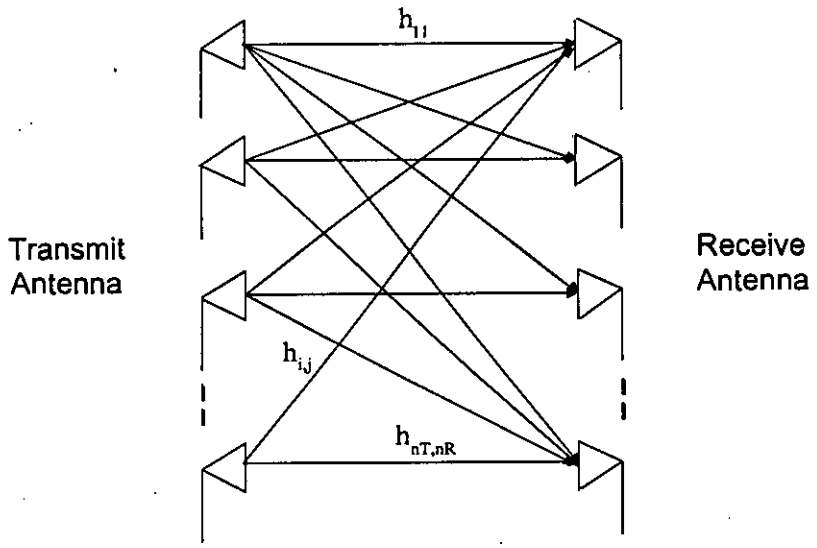

Figure 4.9: Multiple input multiple output channel of wireless network

by symbol x) whereas received signal is represented by an $nR \times 1$ column matrix (denoted by symbol r). The received signal vector,

$$r = Hx + n \tag{4.28}$$

where n is a $nR \times 1$ column matrix of noise at receiving end. Let a matrix is defined as,

$$Q = \begin{cases} HH^H & nR < nT \\ H^H H & nR \geq nT \end{cases} \tag{4.29}$$

The eigenvalues λ of Q is evaluated from,

$$det(\lambda I_m - Q) = 0 \tag{4.30}$$

where, m=min(nR,nT)

Let, another two matrix U and V is defined such that the columns of U are the eigenvectors of HH^H and the columns of V are the eigenvectors of $H^H H$.

Now received signal vectors can be rewritten as,

$$r = UDV^H x + n \tag{4.31}$$

where, D is an $nR \times nT$ non-negative diagonal matrix, U and V are $nR \times nT$ and $nT \times nR$ unitary matrices respectively. So the following transformation,

$$r' = U^H r, \quad x' = V^H x, \quad n' = U^H n$$

The equivalent orthogonal channel i.e. r uncoupled parallel channels would be related like,

$$r' = Dx' + n' \tag{4.32}$$

Here r is the rank of matrix H. Let it is denoted the singular values of H by $\sqrt{\lambda_i}$, $i = 1, 2, 3r$. By substituting the entities $\sqrt{\lambda_i}$ one get,

$$\begin{aligned} r'_i &= \sqrt{\lambda_i} x'_i + n'_i; \quad where \quad i = 1, 2, 3, ...r \\ r'_i &= n'_i; \quad where \quad i = r+1, r+2, r+3, ...nR \end{aligned} \tag{4.33}$$

Uncoupled array antenna system of Equation (4.32) and Equation (4.33) is shown in Figure 4.10.

Now, Channel capacity can be written based on [42],

$$C = W log_2 \sum_{i=1}^{r} (1 + \frac{\lambda_i}{nT} SNR) \tag{4.34}$$

In another form,

$$C = W log_2 \, det(I_m + \frac{Q}{nT} SNR) \tag{4.35}$$

Mean channel capacity could be expressed like [46],

$$E(C) = \int_0^\infty log(1 + \frac{P\lambda}{nT}) \sum_{k=0}^{m-1} \frac{k!}{(k+n-m)!} [L_k^{n-m}]^2 \lambda^{n-m} e^{-\lambda} d\lambda \tag{4.36}$$

where $m = min(nT, nR)$ and $n = max(nT, nR)$, $L_k^{n-m}(x)$ are generalized Laguerre polynomials of order k. In the limit as $nR, nT \rightarrow \infty$, and nR/nT is held constant, the mean capacity converges to [43],

$$E(C) = n\{log(\frac{w}{\sigma^2}) + \frac{1-y}{y} log(\frac{1}{1-y}) - \frac{v}{y}\} \tag{4.37}$$

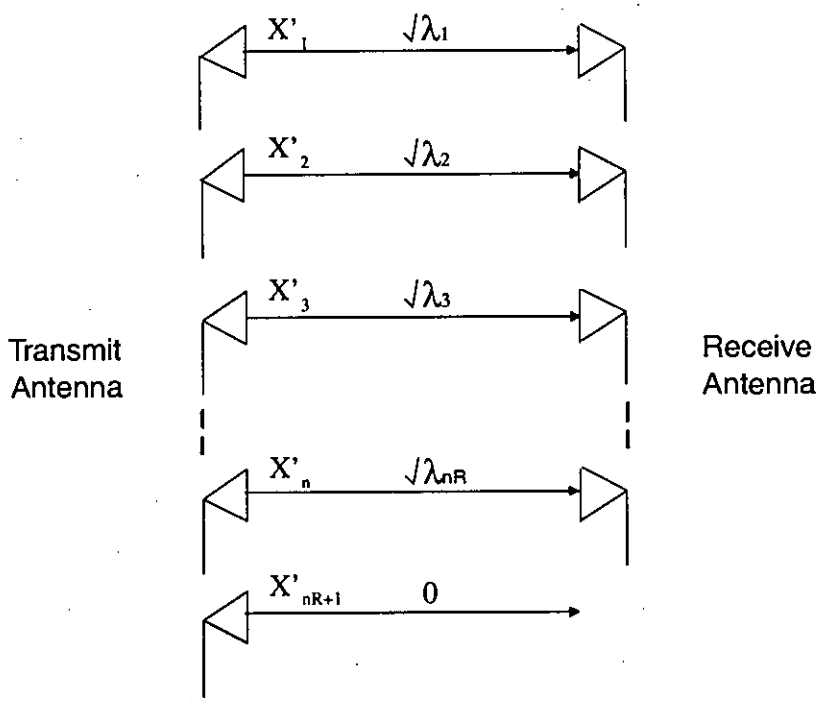

Figure 4.10: Equivalent uncoupled MIMO channel for $nT > nR$

where, $\sigma^2 = 1/P$,$y = nR/nT$,$w = \frac{1}{2}(1 + y + \sigma^2 + \sqrt{(1+\sigma^2)^2 - 4y})$ and $v = \frac{1}{2}(1 + y + \sigma^2 - \sqrt{(1+\sigma^2)^2 - 4y})$

For two transmitting and one receiving antenna case of Figure 4.11, message symbol S_0 and S_1 will be transmitted in first time slot and $-S_1^*$ and S_0^* in second time slot like Table 4.1,

The channel between transmitting and receiving antenna is denoted by [44], $h_0 = a_0 e^{j\theta_0}$ and $h_1 = a_1 e^{j\theta_1}$ where a_i correspond to attenuation of signal and θ_i is the delayed phase of a path. So, Received signal like S. M. Alamouti of [45],

Table 4.1: Symbol sequence of two antenna elements

Time	T_{x1}	T_{x2}
t	X_0	X_1
t+T	$-X_1^*$	X_0^*

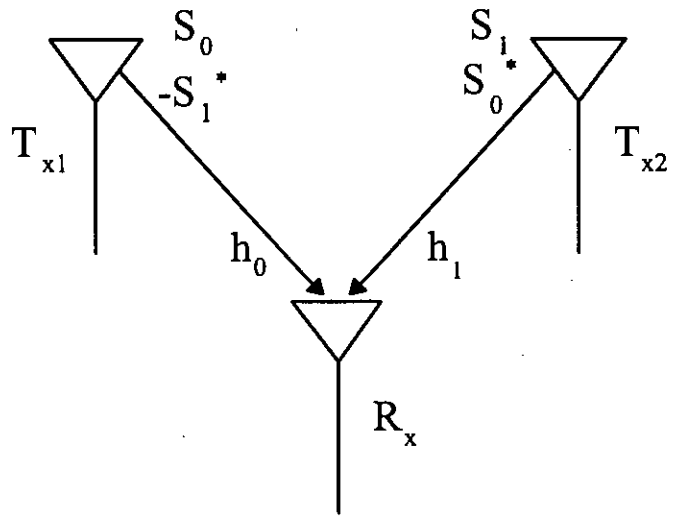

Figure 4.11: Single input multiple output for two antenna case

$$r_0 = r(t) = h_0 S_0 + h_1 S_1 + n_0$$
$$r_1 = r(t+T) = -h_0 S_1^* + h_1 S_0^* + n_1 \tag{4.38}$$

Estimated signal at the combiner output of receiving end is related like,

$$\begin{aligned} S_0 &= [h_0^* \quad h_1][r_0 \quad r_1^*]^T \\ S_0 &= (a_0^2 + a_1^2)S_0 + h_0^* n_0 + h_1 n_1^* \end{aligned} \tag{4.39}$$

$$\begin{aligned} S_1 &= [h_1^* \quad h_0][r_0 \quad -r_1^*]^T \\ S_1 &= (a_0^2 + a_1^2)S_1 - h_0^* n_1 + h_1 n_0^* \end{aligned} \tag{4.40}$$

4.5 Analytical formulation of Throughput

The calculation of the throughput of an OFDM system is more than a simple exercise. In order to calculate the throughput, first convert all of the overheads at each sublayer into a common unit - time. To obtain the maximum throughput (MT), first divide the Medium Access Control (MAC) service data unit (SDU) by the time it takes to transmit it:

$$MT = \frac{MSDU_{size}}{Delay\ per\ MSDU} \tag{4.41}$$

The data rate is not always the same even within the same physical layer convergence protocol (PLCP) protocol data unit (PDU). The data rate of a MAC PDU is determined by its type. Control frames such as request to send (RTS), clear to send (CTS) and acknowledgement (ACK) are always transmitted at 1 Mbps for backward compatibility. The timing diagram is different for carrier sense multiple access/ collision avoidance (CSMA/CA) and RTS/CTS.

The duration of each delay component was determined from the standard [46]. The transmission time of an MAC PDU depends on its size and data rate. The contention window size (CW) does not increase exponentially since there are no collisions. Thus CW is always equal to the minimum contention window size (CW_{min}). The backoff time is selected randomly following a uniform distribution from (0, CW_{min}) giving the expected value of $CW_{min}/2$. Table 4.2 lists the constant and varying delay components.

Table 4.2: Delay components of different MAC schemes

CSMA/CA	T_{DIFS}	T_{SIFS}	T_{BO}	T_{RTS}	T_{CTS}	T_{ACK}	T_{DATA}
OFDM-6	34	9	67.5	N/A	N/A	44^2	$24 \times \lceil 22 + 8 \times (34 + MSDU)/24 \rceil$
OFDM-12	34	9	67.5	N/A	N/A	32^2	$24 \times \lceil 22 + 8 \times (34 + MSDU)/38 \rceil$
OFDM-24	34	9	67.5	N/A	N/A	28^2	$24 \times \lceil 22 + 8 \times (34 + MSDU)/96 \rceil$

The total delay per MSDU is calculated as a summation of all the delay components in the Table 1 as follows:

$$Delay\ per\ MSDU = (T_{DIFS} + T_{SIFS} + T_{BO} + T_{RTS} + T_{CTS} + T_{ACK} + T_{DATA}) \times 10^{-6}\ s \tag{4.42}$$

The total delay per MSDU is simplified to a function of the MSDU size in bytes, x as:

$$Delay\ per\ MSDU(x) = (ax + b) \times 10^{-6}\ s \tag{4.43}$$

One can get the throughput simply by dividing the number of bits in MSDU ($8x$) by the total delay (4). Table 4.3 shows parameters a and b for the throughput formula:

$$MT(x) = \frac{8x}{ax + b} \times 10^6\ bps \tag{4.44}$$

The use of the parameters a and b in the calculation of the throughput for OFDM is based on the assumption that the total delay per MSDU is continuous.

Table 4.3: MT parameters for different MAC schemes

Scheme	Data Rate	a	b
OFDM	6 Mbps	1.33333	223.5
OFDM	12 Mbps	0.66667	187
OFDM	24 Mbps	0.33333	170.75

In fact, the delay is not continuous due to the ceiling operation in the formulae. However, the approximation error due to this operation is relatively small - less than 2% in the worth case.

4.6 OFDM Channel

In order to have a system simulator with acceptable results; a good model for the channel plays an importantrole. This model should consider both the frequency selective fading (channel variation in frequency domain), and Doppler effect (channel variation in time domain).

In a typical in-door environment the received signal is composed of several reflected signals from the walls and other surrounding objects. Any difference in the path length generates a corresponding delay which as a result of high carrier frequency (or small wavelength in comparison with the size of actual elements) generates a random phase with a uniform distribution between zero and 2π. This scenario leads to the Rayleigh fading model. With small movement of the receiver or transmitter, the environmentand reflectors do not change much. But again as a result of small changes in the location of the receiver, the random phases associated with each path change and as a result the gain of the channel changes.

The frequency selective fading behavior of the channel can be model in different ways. The "IMT2000 indoor A channel" [47]mo del can be used for modelling the resolvable multi-paths in the channel. In IMT2000 indoor A channel model, the paths are treated as wide-sense stationary, uncorrelated Gaussian random processes with statistics according to an average power delay profile described by the Table 4.4.

This channel has a fairly flat response with a much higher angle spread. It is assumed that the resolvable multi-path components are within 60^0 with respect to the channel arriving angle of the transmitted signal. The vector channel model

Table 4.4: IMT2000 Indoor A channel

Relative Delay(ns)	Average Power(dB)
0	0
50	-3
110	-10
170	-18
290	-26
310	-32

based on Jake's model is employed to generate the complex amplitude of the resolvable multi-path components for different antenna elements.

$$h_{l,k}(t) = \frac{\sqrt{\overline{P_l}}}{\sqrt{J}} \sum_{i=0}^{J-1} exp\{j[2\pi f_d \cos(\Phi_{l,i})t + \phi_{l,i}]\} exp\{j[\frac{2\pi}{\lambda} d_k \sin(\theta_{l,i})]\} \quad (4.45)$$

where $\overline{P_l}$ is the average power received for the l-th path, J is the number of scatters composing each resolvable path, f_d is the maximum Doppler frequency, $\phi_{l,i}$ is a uniformly distributed random phase, $\Phi_{l,i}$ is the random angle of departure relative to the motion of the mobile of each multipath, d_k is the distance between antenna k and the reference antenna, λ is the carrier wavelength, and $\theta_{l,i}$ is the angle of arrival of each scattered replica with respect to the array normal. Moreover, it is assumed that $\theta_{l,i}$ is distributed as

$$P_{\theta_{l,i}}(x) = \begin{cases} \frac{1}{\Delta_l} & \text{if } \Theta_l - \frac{\Delta_l}{2} \leq x \leq \Theta_l + \frac{\Delta_l}{2} \\ 0 & \text{otherwise} \end{cases} \quad (4.46)$$

where Θ_l and Δ_l are the central angle of arrival and the angle spread of the l-th multipath, respectively. The parameters of the Jake's model for the channel is shown in Table 4.5.

Table 4.5: Parameters for the Jake's model

Name of the parameters	Value
Doppler spread, f_d	10Hz
Number of local scatterers, J	20
Angle spread, Δ	$60^0 (IMT2000)$
Angle of departure, Φ	$0 - 360^0$
Random phase, ϕ	$0 - 360^0$
Normalized distance, d_k/λ	0.5k

It is assumed the channel is quasi-static, meaning that the channel is time-invariant over one OFDM symbol and thus no ICI is introduced to the system. One also assume that the delay spread of the channel is shorter than the guard time and thus ISI is eliminated completely.

4.7 Summary

In this chapter, the maximum ratio combining receiver for multiple receiving antennas are proposed for the OFDM based system. A mathematical model of the proposed system is presented. The BER for the flat fading and frequency selective fading channels for the OFDM based system are calculated and channel capacity and maximum available throughput are also analyzed. Finally OFDM channel used for this thesis work is presented.

Chapter 5

Results and Discussions

In this chapter, simulation results are presented and the performance of multiple antennas are compared.

5.1 System Parameters

In this section, system parameters are listed in tabular forms (Table 5.1 and 5.2) with the value or the types used in the computer simulation.

Table 5.1: OFDM system parameters

Name of the parameters	Value/Type
Number of subcarriers	200
IFFT/FFT period	512
Modulation type	16QAM
Guard period	20
Coding/Decoding	Convolutional Coding / Viterbi decoding
Code rate (R_c)	1/2
Constraint length (K)	7
Interleaver type/depth	Block interleaver / 12×8

For a given bit rate R the parameters of an OFDM system can be determined as follows:

- The OFDM symbol is generated with 512-point inverse FFT (IFFT) and the number of subcarriers that convey information is 200.
- The number of bits per symbol per subcarrier is 4.
- As a rule of thumb, the guard period G should be at least twice as the delay spread τ. To minimize the SNR loss due to the guard period, the

symbol duration should be much larger than the guard period. However, symbols with long duration are susceptible to doppler spread, phase noise, and frequency offset. As a rule of thumb, the OFDM symbol duration T_{sym} should be at least five times as the guard period. Guard period for this simulation is 20.

- It is assumed that the rate of the channel variation is negligibly small over one single burst. In addition, it is assumed to be a coherent 16-QAM with a half-rate convolutional encoding / Viterbi decoding with a constraint length (K) of 7 and a (12×8) block interleaver used in the simulation.

- It is assumed that the receiver is equipped with an eight element ULA with half wavelength spacing between elements. Each element of the antenna array is assumed to be isotropic.

- It is assumed that the frequency is 2.4 GHz. So, wavelength of the channel is $\lambda = 3 \times 10^8/2.4 \times 10^9 = 1/8$. If the velocity is 5km/hr, then doppler spread is $f_d = 100/9$ Hz.

Table 5.2: OFDM channel parameters

Name of the parameters	Value/Type
Maximum doppler spread	100/9 Hz
Sampling frequency	10000 Hz
Number of antenna	2
Mean angle of arrival	30^o
Angle spread of the subpaths	$\pi/3$
Normalized antenna separation	8
Number of unresolved multipath	10

5.2 Performance Comparison

In this section, the performance of the smart antenna with OFDM is presented. The performance criteria is measured by the simulation program and it is done by Matlab programming.

In Figure 5.1, the BER performance is shown for an uncoded OFDM with different number of antennas. As expected, BER performance improves with the increasing number of antennas for the uncoded OFDM. For example, at BER $= 8 \times 10^{-2}$, SNR are 14 dB, 8 dB and 3 dB with 1, 2 and 4 antennas respectively. So performance improvement in SNR is 6 dB for multiple antennas. Hence, the performance of the uncoded OFDM system can be improved for the increasing number of antennas.

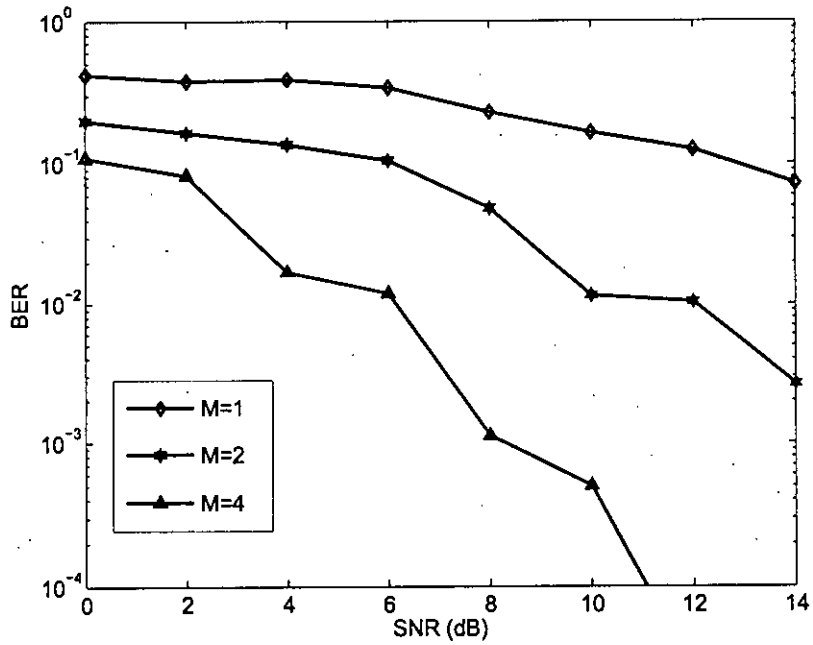

Figure 5.1: BER vs. SNR for OFDM without coding and interleaving for different number of antennas

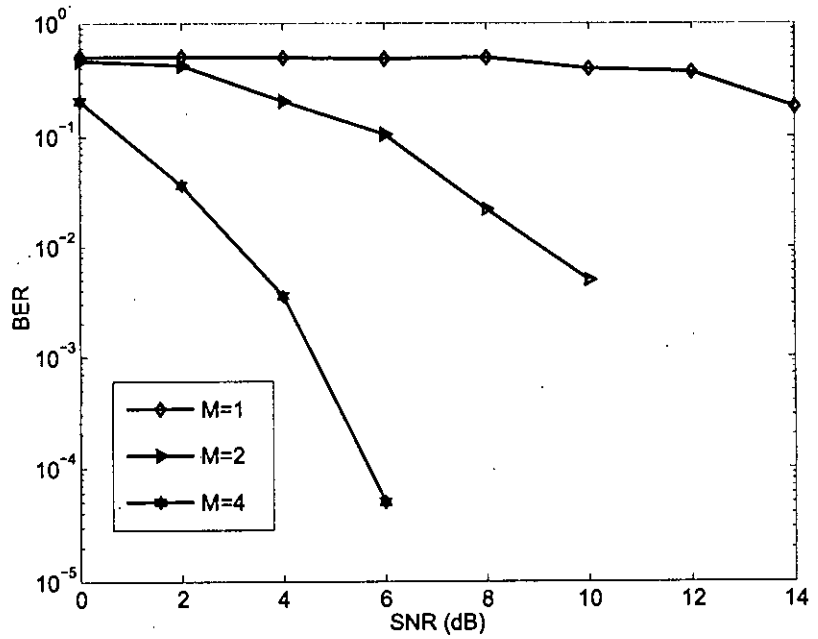

Figure 5.2: BER vs. SNR for coded OFDM with different number of antennas

In Figure 5.2, the BER performance is shown for an coded OFDM with different number of antennas. As expected, the BER performance improves with the increasing number of antennas for coded OFDM. It is seen from the figure that BER is a little improved using single antenna. But using 2 or 4 antenna BER is much improved. For example, at BER $= 5 \times 10^{-1}$, SNR are 14 dB, 4 dB, and 0 dB with 1, 2 and 4 antennas respectively. So there is a 10 dB improvement using multiple antennas instead of single antenna in a coded OFDM system. Hence, the coded OFDM receiver performs better for the increasing number of antennas.

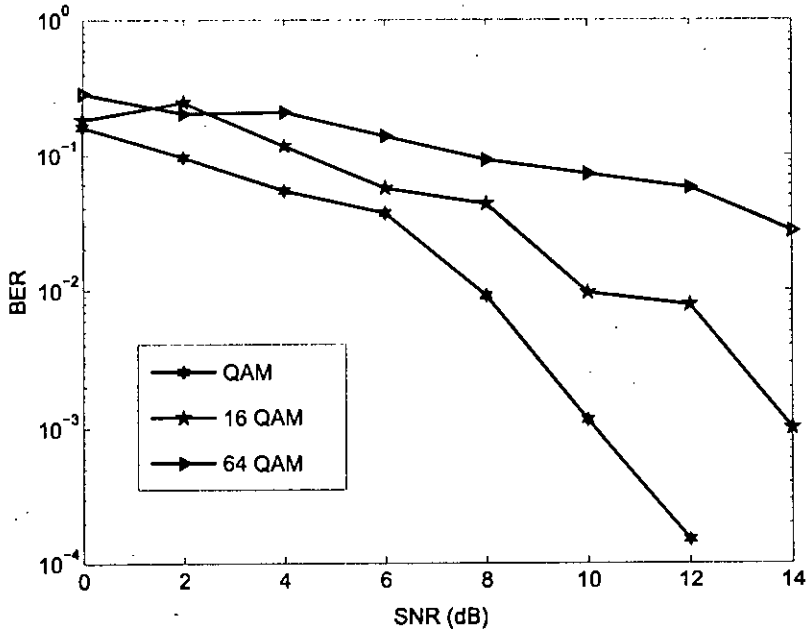

Figure 5.3: BER vs. SNR for different quadrature amplitude modulation for uncoded OFDM with multiple antennas

The BER performance for an uncoded OFDM with different quadrature amplitude modulation schemes is shown in Figure 5.3. With the decrease of constellation points, the BER decreases for uncoded multiple OFDM receivers. This is because the decrease in constellation points, increases the length of two adjacent cell. It is seen in the Figure 5.3 that at the BER $= 5 \times 10^{-2}$, the SNR are 7 dB, 9 dB, and 14 dB with QAM, $16 - QAM$ and $64 - QAM$ respectively.

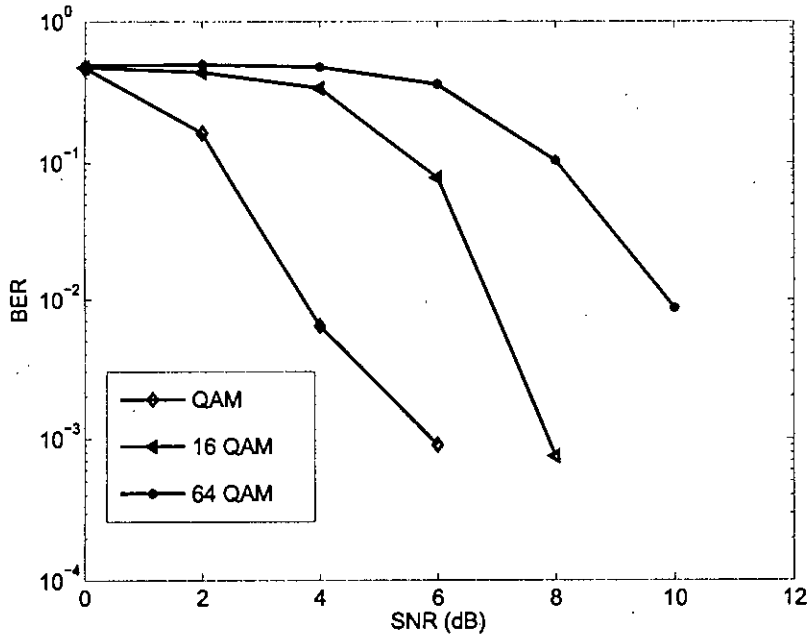

Figure 5.4: BER vs. SNR for different quadrature amplitude modulation for coded OFDM with multiple antennas

In Figure 5.4, the BER performance is shown for the coded OFDM with differentqu adrature amplitude modulation schemes. With the decrease of constellation points, the BER decreases for coded multiple OFDM receivers. This is because with the decrease in constellation points, the length of two adjacent cell is increased. It is seen in the Figure 5.4 that at BER $= 1 \times 10^{-2}$, the SNR are 4 dB, 7 dB, and 10 dB with QAM, $16-QAM$ and $64-QAM$ respectively.

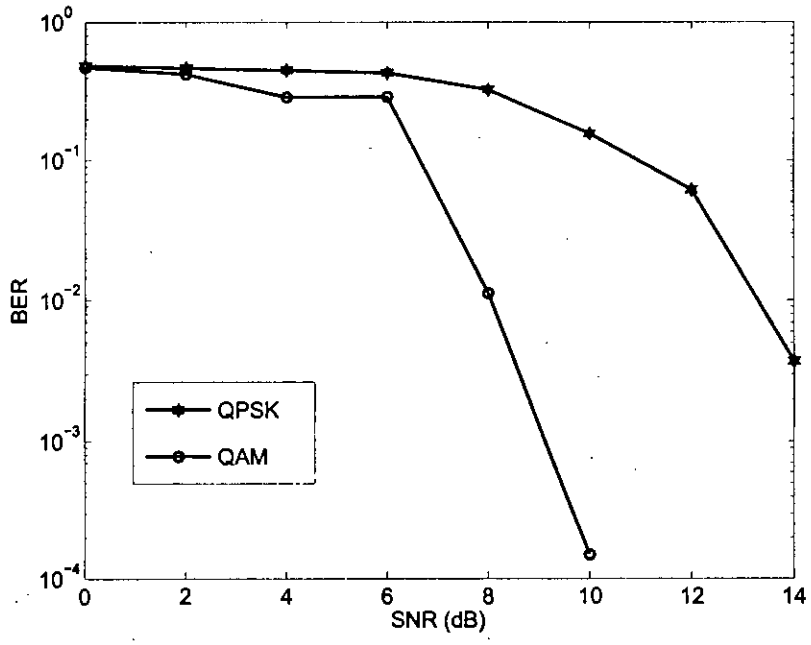

Figure 5.5: BER vs. SNR for different modulation for coded OFDM with multiple antennas

The BER performance for the coded OFDM with different modulation schemes is shown in Figure 5.5. As expected, the BER performance is improved for QAM as compare to QPSK with multiple antennas for the coded OFDM. It is seen in the Figure 5.5 that at BER $= 5 \times 10^{-3}$, the SNR are 8 dB and 14 dB, for QAM and $QPSK$ respectively.

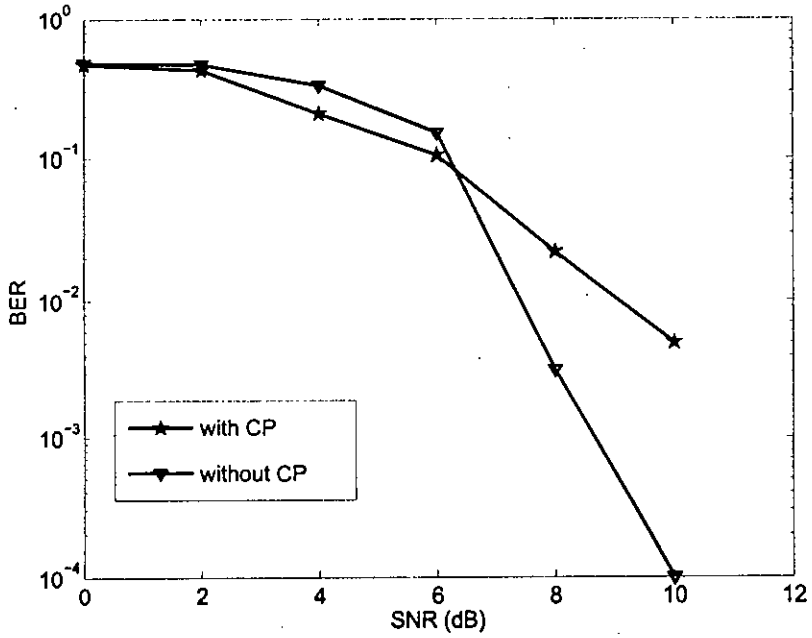

Figure 5.6: BER vs. SNR for different cyclic prefix length for coded OFDM with multiple antennas

In Figure 5.6, the BER is shown for an coded OFDM for different cyclic prefix length. Cyclic prefix is used to mitigate the ISI by the cost of the degradation of BER. This is reflected in the figure. It is seen from the figure that for $BER = 5 \times 10^{-3}$, the SNR are 10 dB and 8 dB, with and without cyclic prefix length.

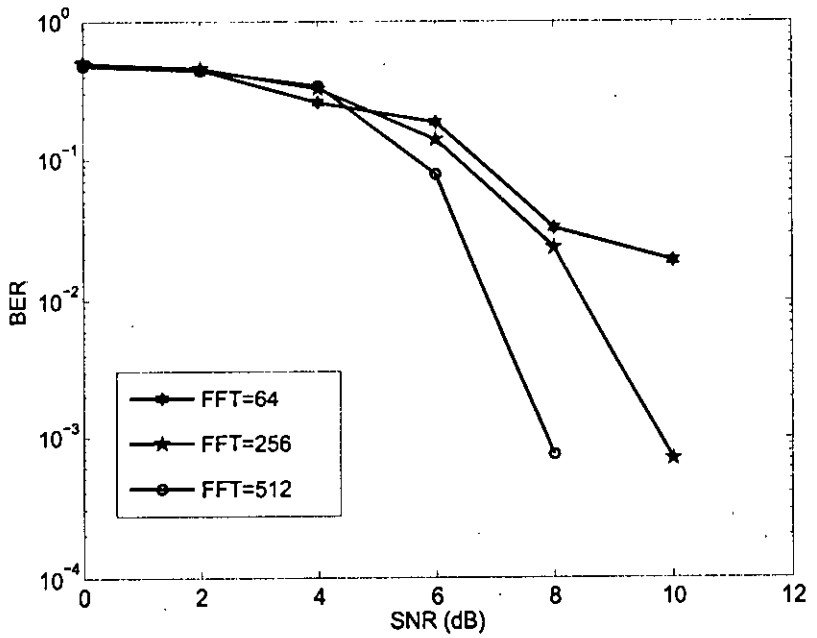

Figure 5.7: BER vs. SNR for different FFT length for coded OFDM with multiple antennas

The BER performance is shown in Figure 5.7 for a coded OFDM for different FFT bin length. From the figure, it is seen that for a particular BER, SNR can be varied by the variation of the FFT bin length. For example, at the BER $= 2 \times 10^{-2}$, the SNR are 10 dB, 8 dB, and 6.5 dB with FFT = 64, FFT = 256 and FFT = 512 respectively. So, the BER performance is improved if FFT bin size is increased with multiple antennas for the coded OFDM.

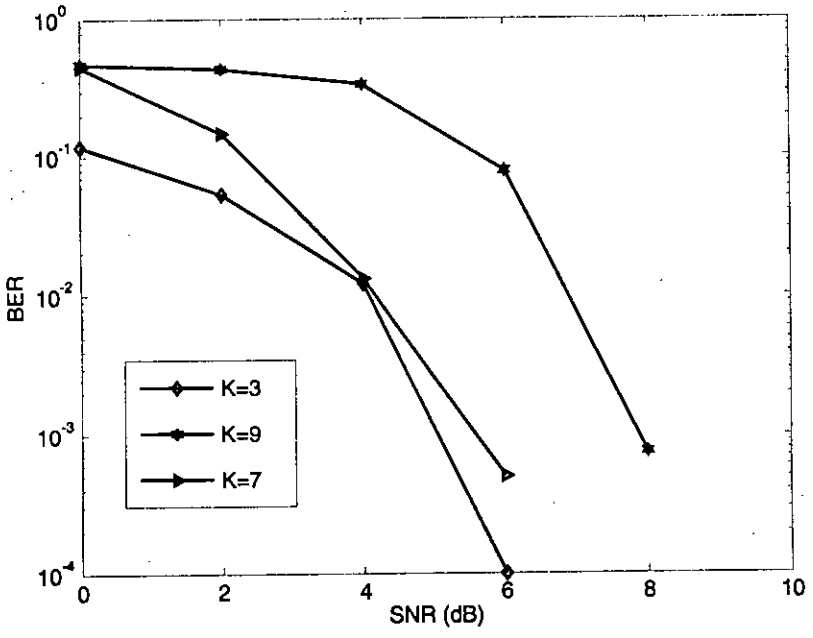

Figure 5.8: BER vs. SNR for OFDM for different constraint length for coded OFDM with multiple antennas

In Figure 5.8, the BER performance is shown for a coded OFDM for differentcons traint length for convolutional code used in the transmitter side of the proposed architecture. From the figure, it is seen that for BER $= 5 \times 10^{-3}$, the SNR is 7 dB, 6 dB and 5.5 dB respectively for constraint length is 3, 7 and 9 respectively. Thus SNR is increased with increased value of the constraint length of the convolutional code.

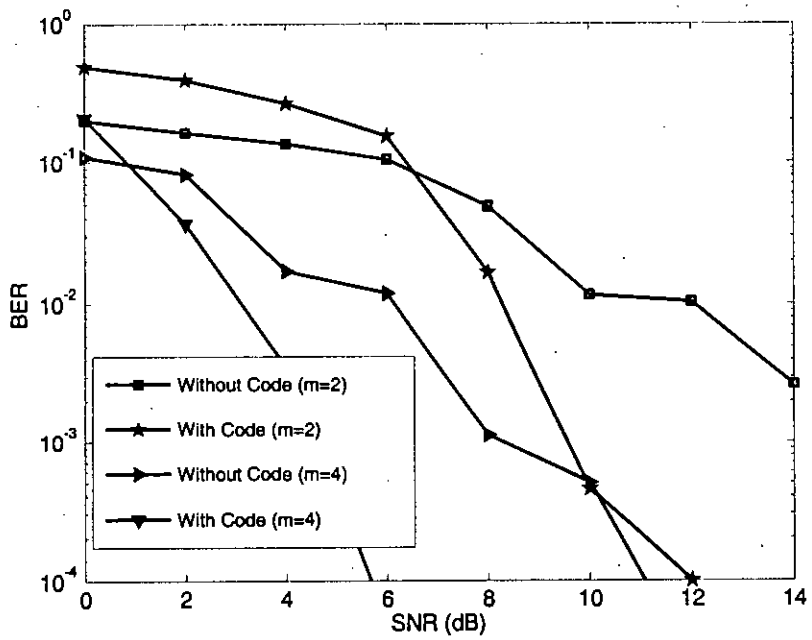

Figure 5.9: BER vs. SNR for OFDM with and without coding and interleaving for multiple antennas

In Figure 5.9, the BER performance is shown for a coded OFDM and an uncoded OFDM for multiple antennas. As expected, the BER performance is improved with the increasing number of antennas. It is also seen in the figure that the BER performance is better for a coded OFDM than an uncoded OFDM. For example, at BER 1×10^{-2}, the SNR are 8 dB and 10 dB for coded and uncoded OFDM respectively, where the number of antennas = 2. Hence, the coded OFDM receiver performs better than the uncoded OFDM for the increasing number of antennas.

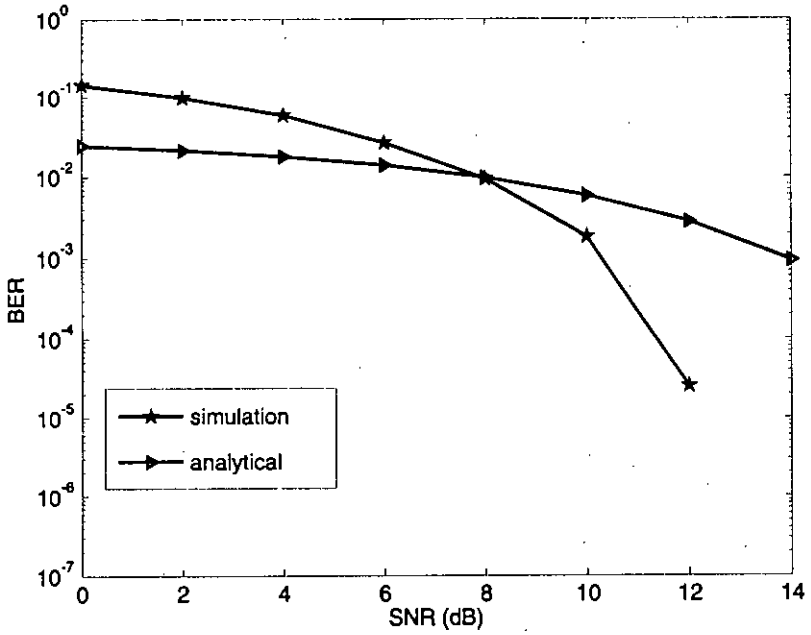

Figure 5.10: BER vs. SNR for OFDM with analytical value and simulation value

In Figure 5.10, the BER performance is shown for the analytical value and the simulation value at the AWGN channel for an OFDM transceiver system. As expected, the BER performance is better for the analytically calculated OFDM system at the low SNR. But at higher SNR, the BER is better for the simulated value. This is because, in analytically calculated BER does not depend on the number of transmitted bits, it only depends on the SNR. But at simulation, the BER depends on SNR and the number of transmitted bits. So in simulation a better performance is achieved when SNR is higher. This is reflected in the figure. For example, at BER 1×10^{-3}, the SNR are 14 dB, for the analytical value but it is 10 dB for the simulation value.

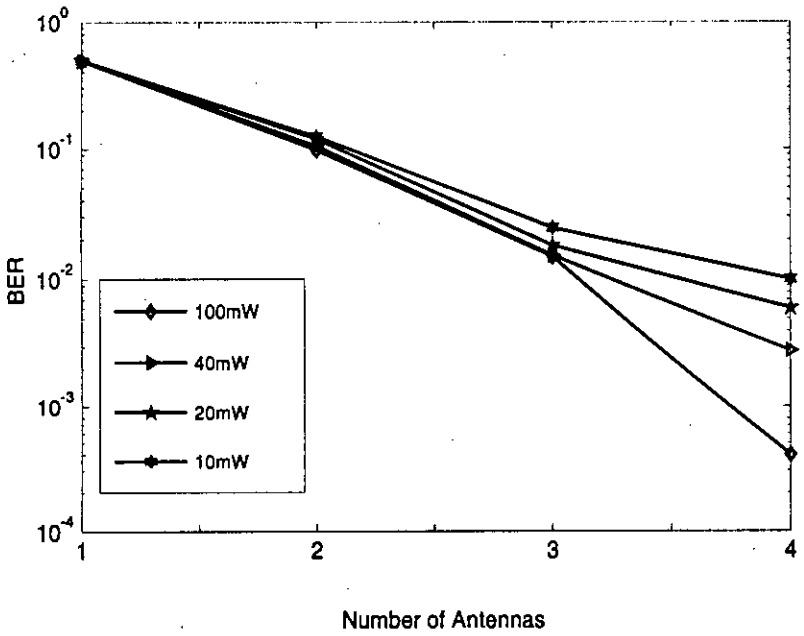

Figure 5.11: BER vs. number of antennas for transmitter power

Figure 5.11 shows the BER vs. number of antennas for power transmitted by the transmitter. As expected, BER is decreased for increasing the number of antennas for a specific transmit power. This is because, when number of antenna is increased BER is decreased. It is also shown from the figure that when transmitter power is increased BER is decreased. This is reflected in the figure. For example, when number of antennas is 4, the BER is 5×10^{-4}, 6×10^{-3}, 8.8×10^{-3}, 1×10^{-2} for transmitter power 100mW, 40mW, 20mW and 10mW respectively.

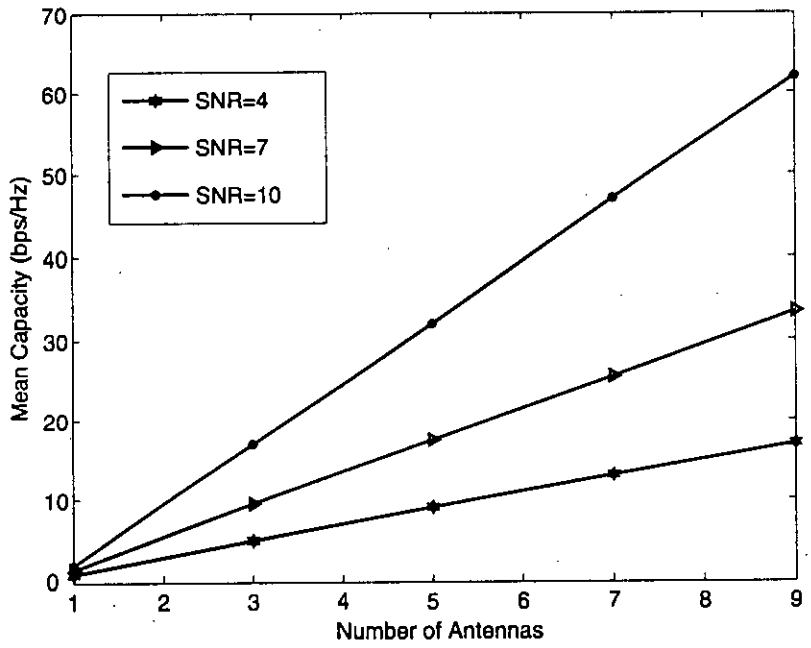

Figure 5.12: Mean channel capacity enhancement by increasing number of antennas

The mean capacity of an OFDM transceiver system is shown in Figure 5.12. As expected, the mean capacity increases due to the increasing number of antennas at a specific SNR. This is because, when number of antenna is increased then mean capacity of the transceiver system is increased. This is reflected in the figure. For example, when number of antenna is 7, at SNR = 4 dB, the mean capacity is 13 bps/Hz. At SNR = 7 dB, the mean capacity is 25.5 bps/Hz and at SNR = 10 dB, the mean capacity is 47 bps/Hz.

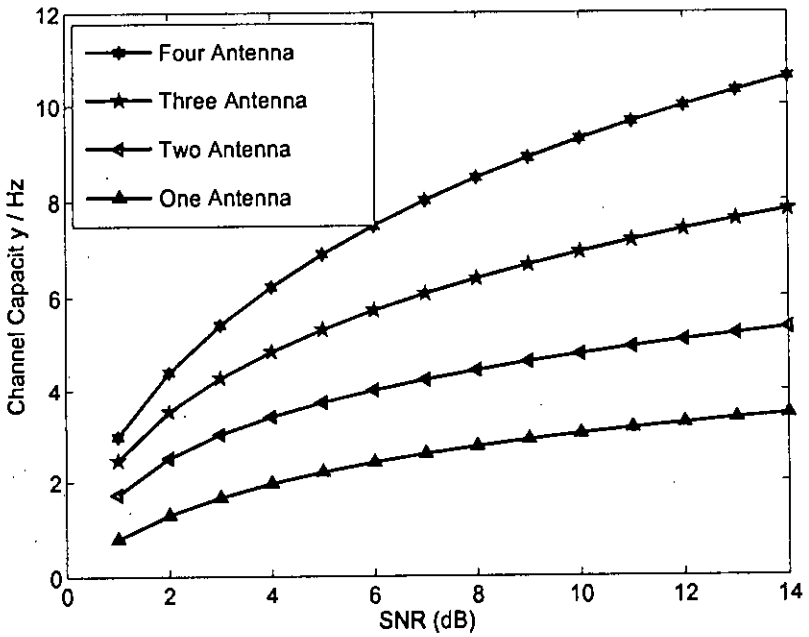

Figure 5.13: channel capacity enhancement by increasing number of antennas

The channel capacity of an OFDM transceiver system is shown in Figure 5.13. As expected, the channel capacity is increased by increasing the number of antennas. This is because, when number of antenna is increased the channel capacity is also increased. This is reflected in the figure. For example, when SNR is 10 dB, the channel capacity is 9/Hz for number of antenna is 4, 7/Hz for number of antenna is 3,5/Hz for number of antenna is 2, 3/Hz for number of antenna is 1.

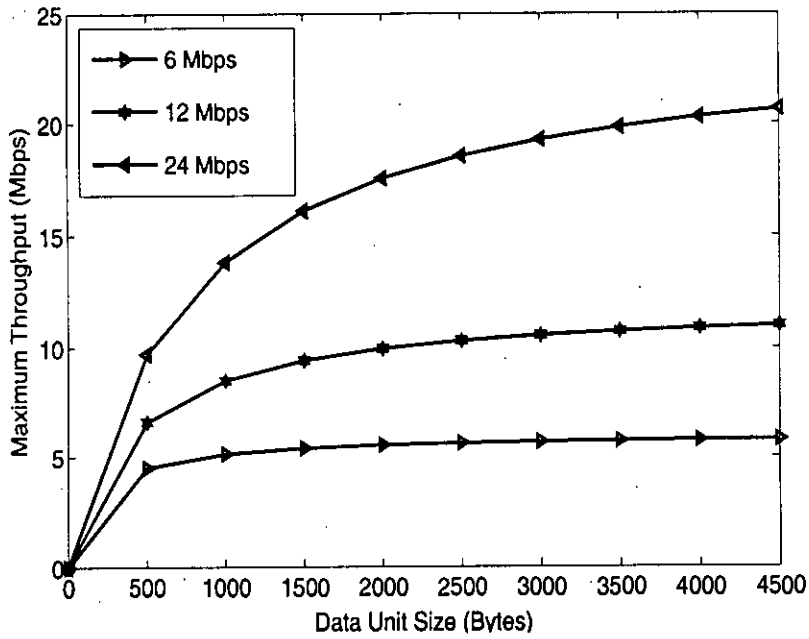

Figure 5.14: Maximum available throughput

The maximum throughput curve for CSMA/CA of an OFDM transceiver system is shown in Figure 5.14. In order to get a clear comparison, the curves are plotted for only the mandatory data rates and the maximum data rate of OFDM. From Figure it is shown that maximum throughput is quite low compared to the basic data rate. When basic data rate is 11 Mbps, data unit is 1500 bytes and CSMA/CA scheme is used, maximum throughput is 5.1 Mbps. Therefore, it is almost impossible to see throughput of over 6.1 Mbps in real deployments where IP packets carrying TCP segments over 1500 bytes are not common. It is also shown that the maximum throughput of higher data rates saturates much later than the maximum throughput of lower data rates.

Chapter 6

Conclusions and Future Work

This chapter summarizes the thesis works and gives future research directions in OFDM based smart antenna systems.

6.1 Conclusions

In this thesis, the performance of smart antennas with OFDM based wireless data network is investigated in vector channel model based on Jack's model. Here, signals received by the multiple receiver antennas are combined by a pre-FFT maximum ratio combiner. The main idea behind MRC is that the output SNR of the combiner is the sum of the SNR of the individual antenna of the OFDM receiver. This is justified by the computer simulation program. Simulation results show that for a particular BER, SNR is improved when the number of antennas is increased. Simulation results also show that the performance of the a coded OFDM is better than uncoded OFDM and QAM performs better than QPSK for multiple number of antennas. Another point is that, in a pre-FFT maximum ratio combiner, signals are combined before FFT processing. Hence the number of FFT blocks is reduced and thus minimizes the complexity of the system. So, the proposed scheme can be used effectively to trade off the system performance and the computational complexity. Moreover, in the proposed OFDM system, the signal power consumption is reduced due to the reduction of the number of FFT blocks and this is an advantage for power critical applications such as low powered wireless devices.

6.2 Future Work

Some possible future research works related to the proposed OFDM system are as follows.

1. This thesis only evaluates the performance of the proposed algorithms for the receiver employing ULA. It may be useful to study its performance for different array geometries, such as the circular array and the planar array.

2. In this thesis, only MRC techniques for OFDM based receiver are presented. It may be possible to use different diversity techniques for OFDM based system. A performance evaluation can also be done with different types of diversity techniques for OFDM based smart antenna systems.

3. In the simulation, the proposed MRC technique is applied for indoor channel model. This technique can also be applied for outdoor channel model like COST-207 six-tap typical urban (TU) channel model.

4. The performance of the system increases as the number of antennas increase. However, the power requirement increases with the increase of the number of antennas. In this thesis, this incremental power consumption is not considered. This effect can be considered for future work.

5. It may be useful to implement the proposed architecture in DSP or in field programmable gate array (FPGA) boards and construct the 8-element array for field trial testing.

Bibliography

[1] B. Van Veen and K. Buckley, *Beamforming: A Versatile Approach to Spatial Filtering*, IEEE ASSP Magazine, pp. 4-22, Apr. 1988.

[2] J. H. Winters, J. Salz, and R. D. Gitlin, *The Impact of Antenna Diversity on the Capacity of Wireless Communication Systems*, IEEE Transactions on Communications, vol. 42, no. 2/3/4, Feb./Mar./Apr. 1994.

[3] R. B. Ertel, *Antenna Array Systems: Propagation and Performance*, Ph.D. Dissertation, Virginia Tech, Jul. 1999.

[4] B. R. Salzberg, *Performance of an Efficient Parallel Data Transmission System*, IEEE Transactions on Communications, vol. COM-15, pp. 805-813, Dec. 1967.

[5] *Orthogonal Frequency Division Multiplexing*, US Patent No. 34884555, filed Nov. 14, 1966, issued Jan. 6, 1970.

[6] S.B. Weinstein, and P. M. Ebert, *Data Transmission by Frequency Division Multiplexing using the Discrete Fourier Transform*, IEEE Transactions on Communications, vol. COM-19, pp. 628-634, Oct. 1971.

[7] B. Hirosaki, *An Orthogonally Multiplexed QAM System using the Discrete Fourier Transform*, IEEE Transactions on Communications, vol. COM-29, pp. 982-989, Jul. 1981.

[8] P. Robertson, and S. Kaiser, *Analysis of the Loss of Orthogonality through Doppler Spread in OFDM Systems*, Global Telecommunications Conference, 1999, GLOBECOM '99, vol. 1b, pp. 701-706, 1999.

[9] Y. Sun, and L. Tong, *Channel Equalization for Wireless OFDM Systems with ICI and ISI*, IEEE International Conference on Communications, ICC.99, vol. 1, pp. 182-186, 1999.

[10] Y. Li, and L. J. Cimini Jr., *Interchannel Interference of OFDM in Mobile Radio Channels*, Global Telecommunications Conference, 2000, GLOBECOM '00, Vol. 2, pp. 706-710, 1999.

[11] F. Bryn, *Optimum Signal Processing of Three-Dimensional Arrays Operating on Gaussian Signals and Noise*, Journal of Acoust. Soc. Am., vol. 34, pp. 289-297, Mar. 1962.

[12] B. Widrow, P. E. Mantey, L. J. Griffiths and B. B. Goode, *Adaptive Antenna Systems*, IEEE Proceedings, vol. 55, No. 12, pp. 2143-2159, Dec. 1967.

[13] H. Boleski, D. Gesbert, and A. J. paulraj, *On the capacity of OFDM-Based Spatial Multiplexing Systems*, IEEE Transactions on Communications, vol. 50, No. 2, pp. 225-234, Feb. 2002.

[14] Y. Li, and N. R. Sollenberger, *Adaptive Antenna Arrays for OFDM Systems with Cochannel Interference*, IEEE Transactions on Communications, vol. 47, No. 2, pp. 217-229, Feb. 1999.

[15] S. Kapoor, D. J. Marchok, and Y. Huang, *Adaptive Interference Suppression in Multiuser Wireless OFDM Systems using Antenna Arrays*, IEEE Transactions on Signal Processing, vol. 47, No. 12, pp. 3381-3391, Dec. 1999.

[16] C. K. Kim, K. Lee, and Y. S. Cho, *Adaptive Beamforming for OFDM Systems with Antenna Arrays*, IEEE Transactions on Consumer Electronics, vol. 46, No. 4, pp. 1052-1058, Nov. 2000.

[17] S. Hara, A. Nishikawa, and Y. Hara, *A novel OFDM Adaptive Antenna Array for Delayed Signal and Doppler-shifted Signal Suppression*, IEEE International Conference on Communications, ICC.2001, vol. 7, pp. 2302-2306, 2001.

[18] M. Budsabathon and Y. Hara, *Optimum Beamforming for Pre-FFT OFDM Adaptive Antenna Array*, IEEE Transactions on vehicular technology, vol. 53, No. 4, pp. 945-955, Jul. 2004.

[19] D. Huang, and K. Letaief, *Pre-DFT Processing using Eigeanalysis for Coded OFDM with Multiple Receive Atennas*, IEEE Transactions on Communications, vol. 52, No. 11, pp. 2019-2027, Nov. 2004.

[20] P. Petrus, *Novel Adaptive Array Algorithms and Their Impact on Cellular System Capacity*, Ph.D. Dissertation, Virginia Tech, Jul. 1997.

[21] P.Zetterb erg, P. Leth-Esperson, And P.Mogens en, *Propagation, Beamsteering and Uplink Combining Algorithms for Cellular Systems*, ACTS Mobile Communications Summit, Royal Institute of Technology, Nov. 1996.

[22] J. C. Liberti, *Analysis of CDMA Cellular Radio Systems Employing Adaptive Antennas*, Ph.D. Dissertation, Virginia Tech, Jul. 1999.

[23] S. P. Stapleton, X. Carbo, and T. Mckeen, *Spatial Channel Simulator for Phased Arrays*, In the Proceedings of the IEEE Vehicular Technology Conference, pp. 1890-1894, 1996.

[24] Q. Spencer, M. Rice, B. Jeffs, and M. Jensen, *A statistical Model for Angle of Arrival in Indoor Multipath Propagation*, In the Proceedings of the IEEE Vehicular Technology Conference, 1997.

[25] W. C. Jakes, ed., *Microwave Mobile Communications*, New York: IEEE Press, 1974.

[26] R.M.Buehrer, A.G. Kogiantis, Shang-Chieh Liu, Jiann-an Tsai and Dirck Uptegrove, *Intelligent Antennas for Wireless Communications Uplink*, Bell Labs Technical Journal, vol 4, pp. 73-103, Jul.-Sep. 1999.

[27] S. U. Pillai, *Array Signal Processing*, Springer-Verlag, New York, 1989.

[28] W. L. Stutzman and G. A. Thiele, *Antenna Theory and Design*, John Wiley & Sons, New York, 1981.

[29] J. Litva and T. K. Lo, *Digital Beamforming in Wireless Communications*, Boston, MA: Artech House, 1996.

[30] T. E. Biedka, *A General Framework for the Analysis and Development of Blind Adaptive Algorithms*, Ph.D. dissertation, Virginia Tech, Oct. 2001.

[31] Z. Rong, *Simulation of Adaptive Array Algorithms for CDMA Systems*, M.S. Thesis, Virginia Tech, Sep. 1996.

[32] Lal C. Godara, *Applications of Antenna Arrays to Mobile Communications, Part I: Performance Improvement, Feasibility, and System Considerations*, Proceedings of the IEEE, Vol. 85, No. 7, Jul. 1997.

[33] A. Peled, and A. Ruiz, *Freuency Domain Data Transmission using Reduced computatioanal complexity algorithms*, Proc. of the IEEE Int. Conf. Acoustics, Speech and Signal Processing, Denver, CO, pp. 964-967, 1980.

[34] A. Czylwik, *Comparison between Adaptive OFDM and Single Carrier Modulation with Frequency Domain Equalization*, VTC 97, vol. 2, pp. 865-869, 1997.

[35] A. Gusmao, R. Dinis, J. Conceicao, and N. Esteves, *Comparison of Two Modulation Choices for Broadband Wireless Communications*, VTC 2000 Spring, vol. 2, pp. 1300- 1305, 2000.

[36] J. Tubbax, B. Come, L. V. der Perre, L. Deneire, S. Donnay, and M. Engels, *OFDM versus Single Carrier with Cyclic Prefix: A System-based Comparison*, VTC 2001 Fall, vol. 2, pp. 1115-1119, 2001.

[37] R. Van Nee and R. Prasad, *OFDM for Wireless Multimedia Communications*, VTC 2001 Fall, vol. 2, pp. 1115-1119, 2001.

[38] M. Dentino, J. McCool, and B. Widrow, *Adaptive Filtering in the Frequency Domain*, Proceedings of IEEE, vol. 66, No. 12, pp. 1658-1659, Dec. 1978.

[39] S. Wicker, *Error Control Systems for Digital Communication and Storage*, Prentice Hall, New Jersey, 1995.

[40] E. R. Berlekamp, *The Technology of Error Correcting Codes*, Proceedings of the IEEE, vol. 68, No. 5, pp. 564-593, May 1980.

[41] I. E. Telatar, *capacity of Multi Antenna Gaussian Channel*, Eur. Trans. Telecom. vol. 10, no. 6, pp. 586-595, Nov/Dec 1999.

[42] P. Smith and M. Shafi, *An Approximate Capacity Distribution for MIMO Systems*, IEEE Transactions on Communications, vol. 52, no. 6, pp. 887-890, Jun. 2004.

[43] P. B. Rapajic and D. Popesu, *Matrix Computations*, IEEE Transactions on Communications, vol. 48, pp. 1245-1248, Aug. 2000.

[44] B. L. Hughes, *Differential Space-Time Modulation*, IEEE Trans. Inform. Theory, vol. 46, no. 7, pp. 2567-2578, Nov. 2000.

[45] Siavash M. Alamouti, *A simple Transmit Diversity Technique for Wireless Communications*, IEEE Journal on Selected Areas in Communications, vol. 16, no. 8, pp. 1451-1458, Oct. 1998.

[46] *Wireless LAN Medium Access Control (MAC) and Physical Layer (PHY) Specification: High-speed Physical Layer Extension in the 2.4 GHz Band*, IEEE standard 802.11, Sep. 1999.

[47] F. Alam, *Simulation of Third Generation CDAM Systems*, M. S. Thesis, Virginia Tech, Dec. 1999.